Conventional sub-soil irrigation techniques do not lower greenhouse gas emission from drained peat meadows

Stefan Theodorus Johannes Weideveld[1*], Weier Liu[2], Merit van den Berg[1], Leon Peter Maria Lamers[1], Christian Fritz[1],

[1] - Aquatic Ecology and Environmental Biology, Institute for Water and Wetland Research, Radboud University, Heyendaalseweg 135, 6525, AJ, Nijmegen, the Netherlands.

[2] - Integrated Research on Energy, Environment and Society, University of Groningen, Nijenborgh 6, 9747 AG, Groningen, the Netherlands

*Corresponding author

E-mail addresses: *Stefan.Weideveld1@gmail.com ,S.Weideveld@science.ru.nl (S.T.J. Weideveld)*

Abstract

Current water management in drained peatlands to facilitate agricultural use, leads to soil subsidence and strongly increases greenhouse gas (GHG) emission. High-density, sub-soil irrigation (SSI) systems have been proposed as a potential climate mitigation measure, while maintaining high biomass production. In summer, SSI was expected to reduce peat decomposition by preventing groundwater tables to drop below -60 cm. In 2017-2018, we evaluated the effects of SSI on GHG emissions (CO_2, CH_4, N_2O) for four dairy farms on drained peat meadows in the Netherlands. Each farm had a treatment site with perforated pipes at 70 cm below soil level spacing 5-6 m to improve both drainage (winter- spring) and irrigation (summer) of the subsoil, and a control site drained only by ditches (ditch water level -60/-90 cm, 100 m distance between ditches). GHG emissions were measured using closed chambers (0.8 x 0.8 m) every 2-4 weeks for CO_2 and CH_4. C inputs by manure and C export by grass yields were accounted for. Unexpectedly, SSI hardly affected ecosystem respiration (R_{eco}) despite raising summer groundwater tables (GWT) by 6-18 cm, and even up to 50 cm during drought. Only when the groundwater table of SSI sites was substantially higher than the control value (> 20 cm), R_{eco} was significantly lower (p<0.01), indicating a small effect of irrigation on C turnover. During wet conditions sub-soil pipes lowered water levels by 1-20 cm, without a significant effect on R_{eco}. As a result, R_{eco} differed little (>3%) between SSI and control sites on an annual base. CO_2 fluxes were high at

all locations, ranging from 35 – 66 and 20 – 50 t CO_2 ha^{-1} yr^{-1} in 2017 and 2018, respectively, even where peat was covered

by clay (25-40 cm). Despite extended drought episodes and lower water levels in 2018, we found lower annual CO_2 fluxes

than in 2017 indicating drought stress for microbial respiration. Contrary to our expectation, there was no difference between

the annual CO_2 fluxes of the sub-soil irrigated (40 and 30 t CO_2–eq ha^{-1} yr^{-1} in 2017 and 2018) and control sites (38 and 34 t

30 CO_2–eq ha^{-1} yr^{-1} in 2017 and 2018). Emissions of N_2O were lower with average emissions were measured (2.9±1.8 mg N_2O.

m^{-2} d^{-1} for 2017) in 2017 than in 2018 (3.6±3.3 mg N_2O. m^{-2} d^{-1}), without treatment effects. The contribution of CH_4 to the

total GHG budget was negligible (<0.1%), with lower GWT favoring CH_4 oxidation over its production. No effect was found

on yields, suggesting that the increased GWT in summer did not increase plant water supply. This is probably because GWT

increase only takes place in deeper soil layers (60-120 cm depth), which also indicates that peat oxidation is hardly affected.

35 We conclude that, although our field-scale experimental research revealed substantial differences in summer GWT and

timing/intensity of irrigation and drainage, SSI fails to lower annual GHG emission and is unsuitable as a climate mitigation

strategy. Future research should focus on potential effects of GWT manipulation in the uppermost organic layers (-30 cm and

higher) on GHG emissions from drained peatlands.

1 Introduction

40 Peatlands cover only 3% of the land and freshwater surface of the planet, yet they contain one third of the total carbon (C)

stored in soils (Joosten and Clarke, 2002). Natural peatlands capture C by producing more organic material than is decomposed

due to waterlogged conditions (Gorham et al., 2012;Lamers et al., 2015). Drainage of peatlands for agricultural purposes leads

to aerobic oxidation of organic material resulting in soil subsidence and the concomitant release of CO_2 and N_2O (Regina et

al., 2004;Joosten, 2009;Hoogland et al., 2012;Lamers et al., 2015;Leifeld and Menichetti, 2018). Soil subsidence occurs when

45 the groundwater table (GWT) drops through drainage, leading to physical and chemical changes of the peat. This results in

consolidation, shrinkage, compaction and increased decomposition (Stephens et al., 1984;Hooijer et al., 2010). Soil subsidence

increases the risk of flooding (frequency and duration) in areas where soil surface subsides below river and sea levels (Syvitski

et al., 2009). In the Netherlands, 26% of the surface area is currently below sea level, an area currently inhabited by 4 million

people (Kabat et al., 2009). This area is expected to increase due to further land subsidence, while sea level is rising at the

50   same time, which is a general issue of coastal peatlands (Erkens et al., 2016). Additionally, peatland subsidence alters

hydrology, leading to drainage problems, salt water intrusion and loss of productive land (Dawson et al., 2010;Herbert et al.,

2015). This will result in strongly increased societal costs and difficulties in maintaining productive land use (Van den Born

et al., 2016;Tiggeloven et al., 2020).

55   The peatland area used for agriculture is estimated at 10% for the USA and 15% Canada, and varies from less than 5 to more

than 80% or Europe (Lamers et al., 2015). In the Netherlands, 85% of the peatland areas are in agricultural use (Tanneberger

et al., 2017), leading to CO_2 emissions of 7 Mt CO_2-eq per year, amounting to 4% of total national greenhouse gas (GHG)

emissions (Arets et al., 2020). Fundamental changes in the management of peatlands are required if land use, biodiversity and

socio-economic values including GHG emission reduction are to be maintained.

60

Carbon dioxide emissions from peatlands are related to the water table position, which affects oxygen intrusion, moisture

content and temperature. There is ample evidence that elevating water levels to 0-20 cm below the land surface results in

substantial reduction of CO_2 emissions from (formerly) managed peatlands (Hendriks et al., 2007;Hiraishi et al.,

2014;Jurasinski et al., 2016;Tiemeyer et al., 2020) Increasing water levels close to the surface not only worsens conditions for

65   aerobic CO_2 production and rapid gas exchange but also reduces land-use intensity (fertilization, tillage, planting, grazing).

Additionally, high water levels favor vegetation assemblages with a higher carbon sequestration potential (e.g. peat forming

plants) compared to common fodder grasses and crops. Experimental research using water table manupulations stresses the

importance of rewetting the upper 20-30 cm to achieve noteworthy CO_2 emissions reduction (Regina, 2014;Karki et al., 2016)

which seems in line with the meta-analysis of field CO_2 emission data by Tiemeyer et al. (2020).

70

Dutch water- and land-authorities have relied on height measurements of the peat surface rather than CO_2 flux measurements

to estimate CO_2 emissions from peatlands (Arets et al., 2020) and the effects of elevated water levels on CO_2 emissions. The

soil-carbon-water model used is based on two assumptions. Firstly, multi-year changes are directly related to carbon losses

from peatlands, eventhough elevation changes are small in magenitude in the range of milimeters per year. Each milimeter of

75   height loss is translated into carbon emissions equalling 2.23 t CO_2 ha^{-1} yr^{-1} (Kuikman et al., 2005;Van den Akker et al., 2010)). Secondly, the average lowest summer GWT is assumed to be a major control of subsidence rates of peat surface elevation and henceforth CO_2 emissions based on the first assumption above (Arets et al. 2020). As a consequence of both assumptions, Dutch climate mitigation frameworks focus on elevating summer GWT in peatlands rather than mean annual GWT (Querner et al., 2012;Brouns et al., 2015). Dutch water- and land-authorities expect that increasing the average lowest summer GWT by

80   20 cm would result in an emission reduction equalling 10.5 t CO_2 ha^{-1} yr^{-1} (Van den Akker et al., 2007;Brouns et al., 2015;Van den Born et al., 2016).

The use of SSI systems has been proposed since the early 2000's (Van den Akker et al., 2010;Querner et al., 2012). SSI works by installing drainage/irrigation pipes at around 70 cm below the surface and at least 10 cm below the ditch water level. Water

85   from the ditch can infiltrate into the adjacent peat and thereby limite GWT drawdowns during summer (c.f. (Hoving et al., 2013), while the pipes also full-fill a drainage function when the GWT is above the ditch water level. Therefore, the SSI was assumed to have an effect of 50% overall reduction of carbon emissions from peatlands (Querner et al., 2012;Van den Born et al., 2016), based on the soil-carbon-water model assumptions that peat layers below -70 cm contribute largely to GHG emissions and that surface elevation differences can be translated directly into CO_2 emissions.

90

The aim of our study was to quantify the effects of SSI on the GWT and the GHG emissions, in particular the net ecosystem carbon balance (NECB). We questioned 1) to what extent can SSI elevate water levels in two summers that differed in drought duration, 2) whether the SSI can substantially reduce (30-50%) CO_2 emission compared to traditional ditch drainage, and 3) whether nitrous oxide peaks are lowered by SSI. To adress these questions we directly compared GHG emissions from a

95   control grassland (traditional ditch drainage) with a treatment grassland (SSI) on four farms over a periode of 2 years (16 site-years).

2 Material and methods

2.1 Study area

The study areas are located in a peat meadow area in the province of Friesland, the Netherlands. The climate is humid Atlantic with an average annual precipitation of 840 mm and an average annual temperature of 10.1°C (KNMI, reference period 1999-2018).

About 62% of the Frisian peatland region is now used as grassland for dairy farming (Hartman et al., 2012). Agricultural land in Friesland is farmed intensively, with high yields, and intensive fertilization (>230 kg N ha^{-1} yr^{-1}). It is characterized by large fields with deep drainage, as one third of the fields are drained to -90 – -120 cm below soil surface. Large parts of these grasslands are covered with a carbon rich clay layer, ranging from 20–40 cm thick. The peat layer below has a thickness of 80–200 cm, which consists of sphagnum peat on top of sedge, reed and alder peat. The top 30 cm of the peat layer is strongly humified (van Post H8-H10) and the peat below 60 – 70 cm deep is only moderately decomposed (van Post H5-H7). On two locations (C and D, see below), there is a 'schalter' peat layer present, highly laminated peat (compacted/ hydrophobic layers of *Sphagnum cuspidatum* remnants) with poor degradability and poor water permeability. The grasslands are dominated by *Lolium Perenne*; other species such as *Holcus lanatus, Elytrigia repens, Ranoculus acris* and *Trivolium repens* are present in a low abundance.

Table 1 Soil and land use characteristics of the research sites in the peat meadows of Friesland, the Netherlands.* Displayed concentrations of the top 70 cm.

Location	Farm type	management	Treatment	Field size ha	mineral top layer thickness m	schalter present	thickness peat layer m	Organic matter g/l	Carbon content kg C-m^2-70cm	C:N*
A	Organic	Grazing	SSI	2	0.35	-	1.6	132.9	53.4	29.2
			Control	0.6	0.40	-	2.0	141.2	47	19.8
B	Conventional	Grazing	SSI	2.3	-	-	1.4	190.7	68.1	34.6
			Control	2.3	-	-	1.4	175.9	74.9	32.8
C	Conventional	Mowing	SSI	1.2	0.30	yes	1.3	141.7	56.3	23
			Control	1.8	0.30	yes	1.0	133.4	60.5	23.5
D	Conventional	Mowing	SSI	2.4	0.30	yes	0.9	161.9	59.6	23.3
			Control	3.5	0.25	yes	0.9	151.5	63.4	26.9
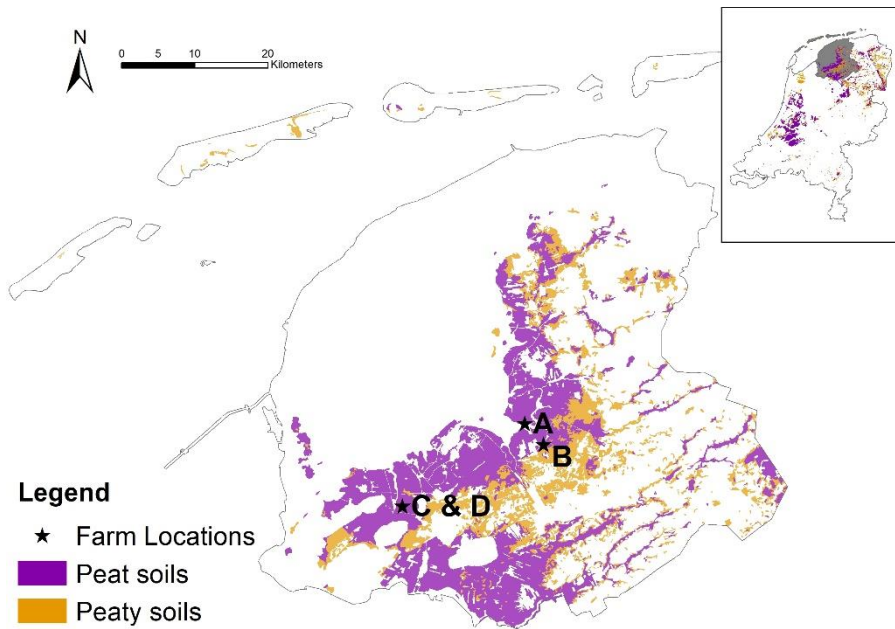
Figure 1 Field locations situated in the province of Friesland, with soil types. Peat soils refer to soils with an organic layer of at least 40 cm within the first 120 cm, while peaty soils are soils with an organic layer of 5-40 cm within the first 80 cm. Insert shows these soil types in the Netherlands, with the location of the field locations in grey.

120 **2.2 Experiment setup**

Four sites were set up at dairy farms with land management and soil types representative for Friesland (see Table 1 and Fig. 1). Each location consisted of a treatment site with SSI pipes and a control site. The irrigation pipes were installed at a depth of 70 cm below the surface and 6 m (2,000 m drains ha^{-1}) apart from each other, except for the D location where pipes were 5 m apart. The pipes were either directly connected to the ditch (A and C) or connected to a collection tube before connected

125 into the ditch (B and D). The connections with ditches were placed 10 cm below the maintained ditchwater level. The control sites are fields that have traditional drainage, through a system with deep drainage ditches (32 – 42 meter from the main ditch) with convex fields and small shallow ditches.

On the treatment sites, three gas measurement frames in 80x80 cm squares were placed for the duration of the experiment on

130 0.5 m, 1.5 m and 3 m distance from the chosen irrigation pipe (Fig. 2), representing best the variation in the environmental conditions and vegetation. Dip well tubes were installed to monitor water levels 0.5, 1.5 and 3 m from the pipe, pairing with the locations of gas measurement frames (Fig. 2). The nylon coated tubes were 5 cm wide and perforated filters placed in the

peat layer. The tube 1.5 m from the irrigation pipe was equipped with a pressure sensor and a data logger (ElliTrack-D, Leiderdorp instruments, Leiderdorp, Netherlands) that measures and records the GWT every hour. Ten more dip well tubes

135 were further placed at intervals 0.5 and 3 m from the pipes in the field, which were manually sampled every 2 weeks during gas sampling campaigns, to obtain the variation on field scale.

Soil samples were taken using a gouge auger three replicas where taken, from 1.5 meter from the irrigation pipes. To determine moisture content, sediment samples were weighed and subsequently oven-dried at105°C for 24 h. Organic matter content was

140 determined via loss on ignition. Dried sediment samples were incinerated for 4 h at 550°C (Heiri et al., 2001). Total nitrogen (TN) and total carbon (TC) was determined in soil material (9-23 mg) using an elemental CNS analyzer (NA 1500, Carlo Erba; Thermo Fisher Scientific, Franklin, USA)

Soil temperature at -5, -10 and -20 cm depth and soil moisture were continuously measured (12-Bit Temperature sensor -S-

145 TMB-M002 and 10HS Soil Moisture Smart Sensor, Onset Computer Corporation, Bourne, USA) and recorded every 5 min on a data logger (HOBO H21-USB Micro Station Onset Computer Corporation, Bourne, USA). Because of the frequent failure of sensors, extra temperature sensors (HOBO™ pendant loggers, model UA-002-64, Onset Computer Corporation, Bourne, USA) were placed in the soil at a depth of -10 cm.

150 At farms A and D, sensors were set up at 1.5 m above ground to measure photosynthetically active radiation (PAR, Smart Sensor S-LIA-M003, ONSET Computer Corporation, Bourne, USA), air temperature and air humidity (Temperature/Relative Humidity Smart Sensor, S-THB-M002, Onset Computer Corporation, Bourne, USA). Data were logged every 5 minutes (HOBO H21-USB Micro Station, Onset Computer Corporation, Bourne, USA). Average air temperature and precipitation from the weather station Leeuwarden (18 to 30 km distance from research sites) were used. (KNMI, data). The location specific

155 precipitation was estimated using radar images with a resolution of 3x3 km
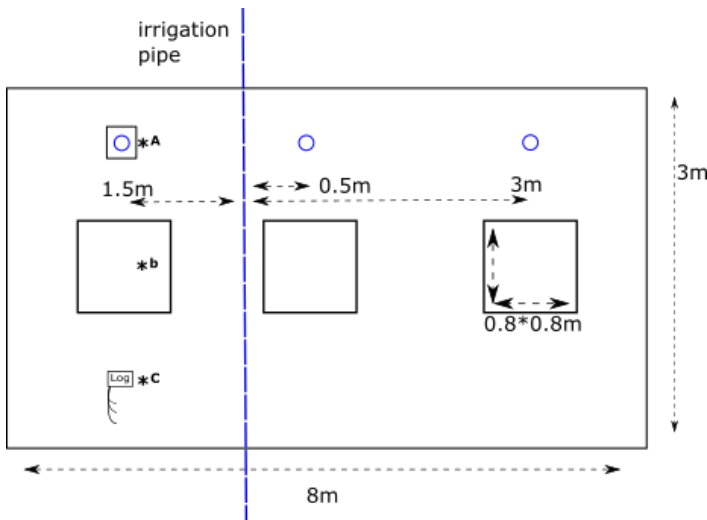
Figure 2 Overview field site SSI. Blue dashed line = irrigation pipe, blue circle = dipwell, A – dipwell with data logger, B – gas measurement frame, C – data logger, -5 -10 -20 soil temperature and soil moisture

C-export was determined by harvesting the frames eight times in 2017 and five times in 2018, the whole field site were managed with 4-5 cuts per year to have a similar grass height with the surrounding field. The biomass was harvested where weighed and dried at 70 °C until constant weight. Total nitrogen (TN) and total carbon (TC) was determined in dry plant material (3 mg) using an elemental CNS analyzer (NA 1500, Carlo Erba; Thermo Fisher Scientific, Franklin, USA)Due to grazing disturbance in 2018, an estimation instead of measurements was made for the C-export of location A in consultation with the farmer, but excluded from statistical analysis. Four times per year slurry manure from location C was applied to all plots. The slurry was diluted with ditchwater (2:1 ratio) and applied above ground in the gas measurement frames and the surrounding area. (119 – 181 kg N ha^{-1} yr^{-1} for 2017 and 129 – 162 kg N ha^{-1} yr^{-1} for 2018 with a C/N ratio of 16.3±1.3

2.3 Flux measurements

CO_2 exchange was measured from January 2017 to December 2018, at a frequency of two measurement campaigns a month during growing season (April – October) and once a month during winter. This resulted in 34 (A), 35 (C and D) and 38 (B) campaigns over the two years for CO_2 and CH_4. The N_2O emissions where measured with a lower frequency with 22 (A), 20 (B and C) and 17 (D) campaigns over the two years.. A measurement campaign consisted of flux measurements with opaque (dark) and transparent (light) closed chambers (0.8x0.8x0.5 m) to be able to distinguish ecosystem respiration (R_{eco}) and gross

primary production (GPP) from net ecosystem exchange (NEE). During winter an average of 9 light and 10 dark measurements, and during summer 18 light and 20 dark measurements were carried out over the course of the day, to achieve data over a gradient in soil temperature and PAR.

175   The chamber was placed on a frame installed into the soil and connected to a fast greenhouse gas analyzer (GGA) with cavity ring-down spectroscopy (GGA-30EP, Los Gatos Research, Santa Clara, CA, USA) to measure CO_2 and CH_4 or to a G2508 gas concentration analyzer with cavity ring-down spectroscopy (G2508 CRDS Analyzer, Picarro, Santa Clara, CA, USA) to measure N_2O. To prevent heating and to ensure thorough mixing of the air inside the chamber, the chambers where equipped with two fans running continuously during the measurements. For CO_2 and CH_4, each flux measurement lasted on average

180   180s. N_2O fluxes were measured on all frames at least once during a measurement campaign, with an opaque chamber for 480s per flux.

    PAR was manually measured (Skye SKP 215 PAR Quantum Sensor, Skye instruments Ltd, Llandrindod Wells, United Kingdom) during the transparent measurements, on top of the chamber. The PAR value was corrected for transparency of the

185   chamber. Within each measurement, a variation in PAR higher than 75 $\mu mol\ m^{-2}\ s^{-1}$ would lead to a restart of the measurement. Soil temperature was measured manually in the frame after the dark measurements at -5 and -10 cm depth (Greisinger GTH 175/PT Thermometer, GMH Messtechnik GmbH, Regenstauf, Germany). Crop height was measured using a straight scale with a plastic disk with a diameter of 30 cm before starting the measurement campaign.

 2.4 Data analyses

2.4.1 Flux calculations

Gas fluxes were calculated using the slope of gas concentration over time (Almeida et al., 2016) (eq.1).

$$F = \frac{V}{A} * slope * \frac{P * F1 * F2}{R * T}$$

(1)

Where F is gas flux (mg m^2 d^{-1}), V is chamber volume (0.32 m^3), A is the chamber surface area (0.64 m^2), slope is the gas concentration change over time(ppm $second^{-1}$); P is atmospheric pressure (kPa); F1 is the molecular weight, 44 g mol^{-1} for CO_2 and N_2O and 16 g mol^{-1} for CH_4; F2 is the conversion factor of seconds to days; R is gas constant (8.3144 J K^{-1} mol^{-1}); and T is temperature in Kelvin (K) in the chamber.

2.4.2 R_{eco} modeling

To gap-fill for the days that were not measured for an annual balance for CO_2 exchange, R_{eco} and GPP models needed to be fitted with the measured data for each measurement campaign. R_{eco} was fitted with the Lloyd-Taylor function (Lloyd and Taylor, 1994) based on soil temperature (Eq. 2):

$$R_{eco} = R_{eco,Tref} * e^{E_0*\left(\frac{1}{T_{ref}-T_0}-\frac{1}{T-T_0}\right)}$$

(2)

where R_{eco} is ecosystems respiration, $R_{eco,Tref}$ is ecosystem respiration at the reference temperature (T_{ref}) of 281.15 K and was fitted for each measurement campaign, E_0 is long term ecosystem sensitivity coefficient (308.56, (Lloyd and Taylor, 1994)), T_0 Temperature between 0 and T (227.13, Lloyd and Taylor, 1994), T is the observed soil temperature (K) at 5 cm depth and T_{ref} is the reference temperature (283.15 K). If it was not possible to get a significant relationship between the T and the R_{eco} with data from a single campaign, data were pooled for two measuring days to achieve significant fitting (Beetz et al., 2013;Poyda et al., 2016;Karki et al., 2019)

2.4.3 GPP modeling

GPP was obtained by subtracting the measured R_{eco} (CO_2 flux measured with the dark chambers) from the measured NEE (CO_2 flux measured with the light chambers) according to measurement time. For the days in between the measurement

campaigns, data were modeled with the relationship between the GPP and PAR using a Michaelis–Menten light optimizing

215   response curve (Beetz et al., 2013;Kandel et al., 2016). For each measurement location per measurement campaign, the GPP

was modeled by the parameters α and GPP_{max} (maximum photosynthetic rate with infinite PAR) of (eq.3):

$$GPP = \frac{\alpha * PAR * GPP_{max}}{GPP_{max} + \alpha * PAR}$$

(3)

220   where NEE is the measured CO_2 flux with light chamber, α is ecosystem quantum yield (mg CO_2 - C m^{-2} h^{-1})/(µmol m^{-2} s^{-1})

which is the linear change of GPP per change in PAR at low light intensities (<400 µmol m^{-2} s^{-1} as in (Falge et al., 2001), PAR

is measured photosynthetic active radiation (µmol quantum m^{-2} s^{-1}), GPP_{max} is gross primary productivity at its optimum. Due

to low coverage of the PAR range in a single measurement campaign, data from multiple campaigns were pooled according

to dates, vegetation, and air temperature.

225   **2.4.4 NECB calculations**

The NEE is the sum of R_{eco} and GPP values, calculated by applying the hourly monitored soil temperature and PAR data to

the models developed per campaign. Extrapolated values at times between two adjacent models are weighted averages of the

estimates from these two models, where the weights are temporal distances of the extrapolated time spots to both of the

measurements. To account for the influence from plant biomass on the CO2 fluxes, linear relationships between grass height

230   and model parameters ($R_{eco,Tref}$, GPP_{max}, and α) were developed. Models developed for the campaign before harvesting were

then corrected using the slopes of the linear regressions as the models after the harvest to be applied in the extrapolation.

Unrealistic parameters after correction were discarded, and instead adopted from parameters from campaigns with low grass

height at the same plot. The annual CO_2 fluxes were thus summing of the hourly R_{eco}, GPP and NEE values.The atmospheric

sign convention was used for the calculation of NECB. All C fluxes into the ecosystem where defined as negative (uptake

235   from the atmosphere into the ecosystem), and all C fluxes from the ecosystem to the atmosphere are defined as positive. This

also holds for non-atmospheric inputs like manure (negative) and outputs like harvests (positive). Both harvest and manure

input are expected to be released as CO_2.

2.4.5 CH$_4$ and N$_2$O fluxes

CH$_4$ and N$_2$O fluxes per site and measurement campaign were averaged per day. The annual emissions sums for CH$_4$ where

240   estimated by linear interpolation between the single measurement dates. Global Warming Potential (GWP) of 34 t CO$_2$-eq and

N$_2$O was used according to IPCC standards (Myhre et al., 2013) to calculate the yearly GHG

balance.

2.4.6 Uncertainties

The estimation of total uncertainties of the yearly budget should include multiple sources of error, where both model error and

245   uncertainty from extrapolations in time are the most important (Beetz et al., 2013). Therefore, we included these two sources

of error and combined them into a total uncertainty in three steps. First, we calculated the model error, which would cover the

uncertainties from replications (between the three frames) and the random errors from the measurements, the environmental

conditions at the time, and the parameter estimation of R$_{eco}$ and GPP. Standard errors (SE) of the prediction were calculated

for each measurement campaign / pooled dataset as the SEs of the midday of the campaign dates. The hourly SEs were then

250   extrapolated linearly between modeled campaigns. Total model error of the annual NEE was therefore calculated following

the law of error propagation as the square root of the sum of squared SEs. Second, we attribute the uncertainty from

extrapolation to the variations from selecting different gap-filling strategies, since other approaches of annual NEE estimation

including different R$_{eco}$ and GPP models would result in different values (Karki et al., 2019).. To quantify this uncertainty, six

R$_{eco}$ models and four GPP models were select from Karki et al. (2019)) and fitted with annual data (Appendix Table A1). The

255   models were evaluated following the thresholds of performance indicators in Hoffmann et al. (2015). R$_{eco}$ and GPP models

that were above the 'satisfactory' rating was accepted and calculated into gap-filled NEEs. Based on all the annual NEEs per

site and year, standard deviations from the means were considered as the extrapolation uncertainty. In the year 2018, the control

site of farm D did not yield any satisfactory R$_{eco}$ model. The uncertainty was thus calculated as the average of all sites.

Finally, we calculated the total uncertainties per site and year following the law of error propagation with the uncertainties

260   from the previous steps.

2.5 Statistics

The effect of the treatment on gap-filled annual R_{eco} and GPP, the resulting NEE, the C-export data, the NECB, and the measured CH_4, N_2O exchanges were tested by fitting linear mixed-effects models, with farm location as a random effect. Effectiveness of the random term was tested using the likelihood ratio test method. Significance of the fixed terms was tested via Satterthwaite's degrees of freedom method. General linear regression was used instead when the mixed effect model gives singular fit. The treatment effect was further tested using campaign-wise R_{eco} data. Measured R_{eco} fluxes from SSI and Control were calculated into daily averages and paired per date. The data pairs were grouped based on the GWT differences between SSI and control of the dates. Differences between treatments were then analyzed by linear regression of the R_{eco} flux pairs without interception and testing the null hypothesis 'slope of the regression equals to 1'. All statistical analyses were computed using R version 3.5.3 (Team, 2019) using packages lme4 (Bates et al., 2014), lmerTest (Kuznetsova et al., 2017), sjstats (Lüdecke, 2019), and car (Fox and Weisberg, 2018).

3 Results

3.1 Weather conditions

275   Mean annual air temperature was 10.3 ℃ for 2017 and 10.7 ℃ for 2018, which were higher than the 30-year average of 10.1

℃. The growing season (April–September) in 2017 was slightly cooler with 14.3 ℃ than the average of 2018 at 14.6 ℃, while

the temperature during the growing season in 2018 was 1.1 ℃ warmer than average. Precipitation was slightly higher for 2017

840-951 mm compared to the 30-year average of 840 mm (KMNI). There was a small period of drought in May and June,

ending in the last week of June (see Fig.3). In contrast, 2018 was a dry year with average of 546-611 mm. The year is

280   characterized by a period of extreme drought in the summer, from June to the beginning of August, and precipitation lower

than average in the fall and winter.
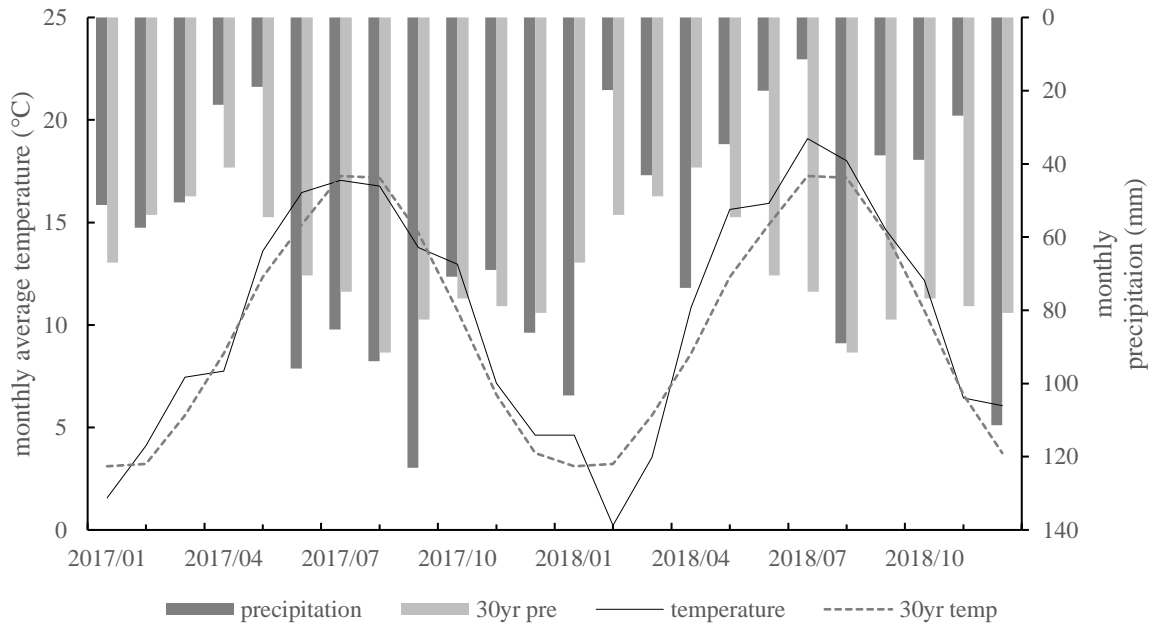
Figure 3 Monthly average air temperature at weather station Leeuwarden (18 to 30 km distance from research sites), and the 30-
285   **year average. Sum precipitation at weather station Leeuwarden, and the 30-year average.**
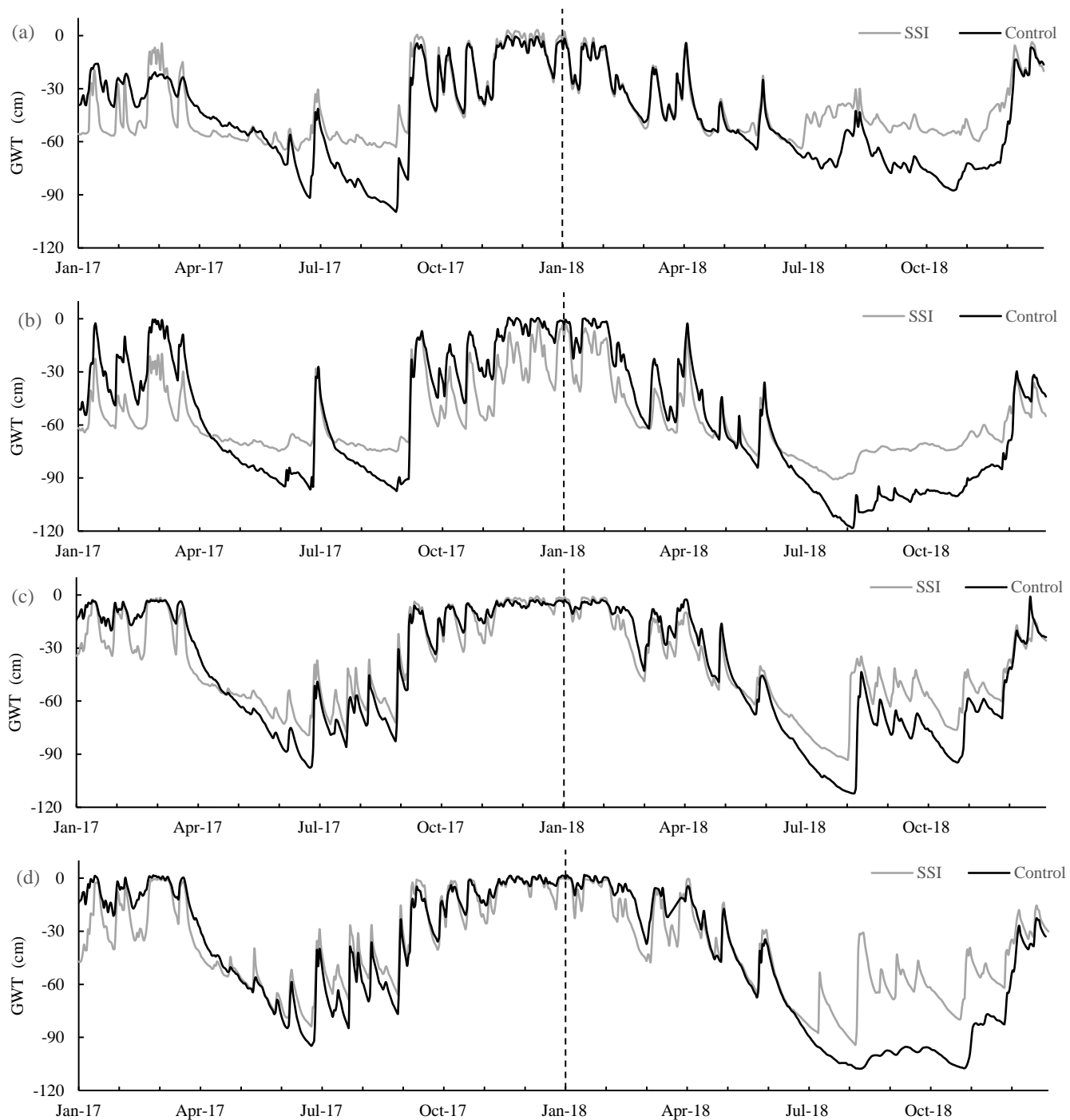
Figure 4 Groundwater table (GWT, from soil surface) during the measuring period per farm (letter), per graph SSI (measured 1.5 m from the irrigation pipe) and control.

3.2 Groundwater table (GWT)

Deploying SSI systems affected the GWT during the two years for all farms (Fig. 4). However, there was a large variation in effect-size between years and locations. The effect of SSI can be divided into two types of periods. Periods with drainage (decreased GWT), in the wet periods, coincided with the autumn (in 2017) and winter period (2017 and 2018). Irrigation (increased GWT) periods, where the SSI leads to a higher water table than control, occurred during spring and summer when the GWT dipped below the ditch water level. In 2017, the effectiveness differed per farm. For locations A and B, GWT was more stable in summer around the -60 and -70 for SSI compared to the control, while locations C and D the GWT fluctuated more like in the control fields. During the dry summer of 2018, in contrast, all locations showed a strong effect of irrigation, especially after the dry period in the beginning of august. In this period the water table recovered quickly while the control lagged behind.
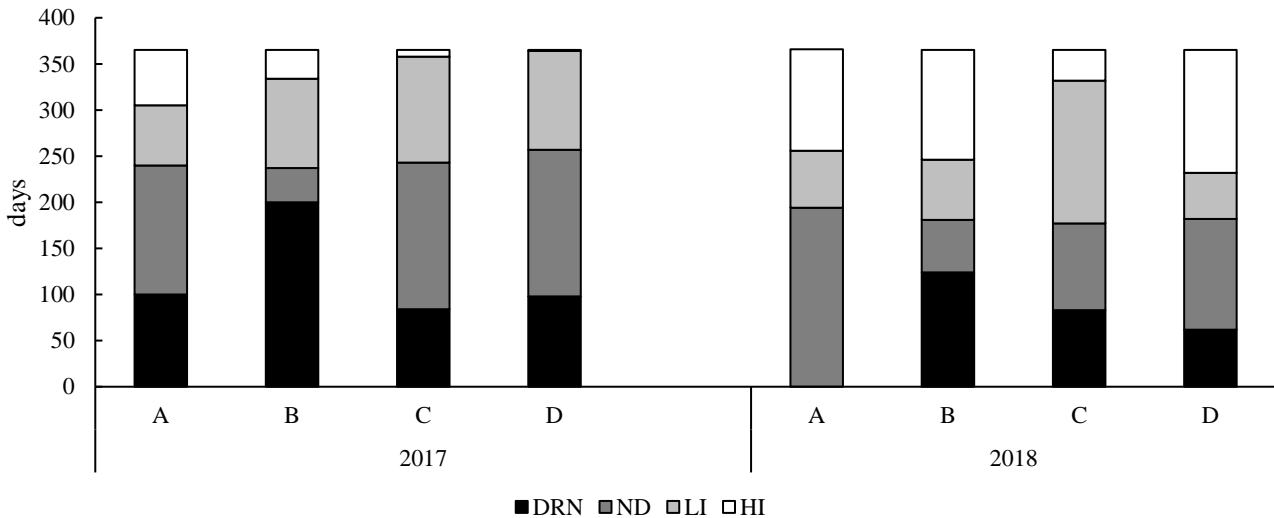
Figure 5 Days with effective drainage/ irrigation for the four locations. drainage (DRN, <-5 cm), no difference (ND, -5 ~ 5 cm), low to intermediate irrigation (LI, 5 ~ 20 cm) and high irrigation (HI, > 20 cm) 1.5 m from the irrigation pipe.

Although there was hardly any difference in annual average GWT between control and SSI (Table 2), drainage and irrigation effects could be observed when dividing the calendar year into seasons. The effective days of the SSI are summarized in Fig. 5 according to four categories, based on practical definitions of drainage and irrigation: drainage (DRN, <-5 cm), no difference (ND, -5 ~ 5 cm), low to intermediate irrigation (LI, 5 ~ 20 cm) and high irrigation (HI, > 20 cm). These categories are also

used in the statistical analysis of R_{eco} measurements (see 3.7 Seasonal R_{eco}). In 2017 there were 17 days more without any GWT difference than in 2018. There was a much stronger irrigation effect in the dry year of 2018, with 61 more irrigated days

310 comparing to 2017, and the number of irrigation days was constantly similar to, or higher than the number of drainage days, except for site B in 2017 which had a long period showing a drainage effect.

Table 2:Average groundwater table during the measuring period per farm. Summer groundwater table ranges from April till October. Measured 1.5 meter from the irrigation pipe.

Location	Treatment	Average 2017	Summer 2017	Average 2018	Summer 2018
A	SSI	-43	-52	-51	-48
	Control	-40	-63	-41	-59
B	SSI	-47	-64	-67	-71
	Control	-53	-73	-61	-83
C	SSI	-35	-54	-51	-56
	Control	-34	-61	-45	-67
D	SSI	-31	-51	-59	-56
	Control	-32	-56	-45	-77

315 **3.3 Measured R_{eco}**

Fig. 6 compares the measured R_{eco} fluxes with the corresponding GWT measurements, which could give an indication for the effectiveness of the GWT differences. The division between the groups was based on the GWT differences between the SSI and control sites on the measurement days (the same groups used in Fig. 5). There was a slightly higher R_{eco} for SSI during drainage periods when GWT was lower, which compensates for the lower R_{eco} during summer. For moments where there was

320 no GWT difference and those showing moderate irrigation, there was no effect of SSI on R_{eco}. However, when the GWT of the SSI was more than 20cm higher than the control, the emissions of the control where significantly higher than SSI ($p <$ 0.01), indicating an effect of the irrigation. However, this effect of the raised GWT was small, even though in some cases the GWT was raised more than 60 cm. According to Fig. 5, in 2017, the majority of the days were dominated by drainage (increasing R_{eco}), or by no difference or small irrigation resulting in no effect on the R_{eco}. However, the moments with increased

325 irrigation, when there was a reduced R_{eco} effect of SSI, were sparse compared to the other dominating periods.
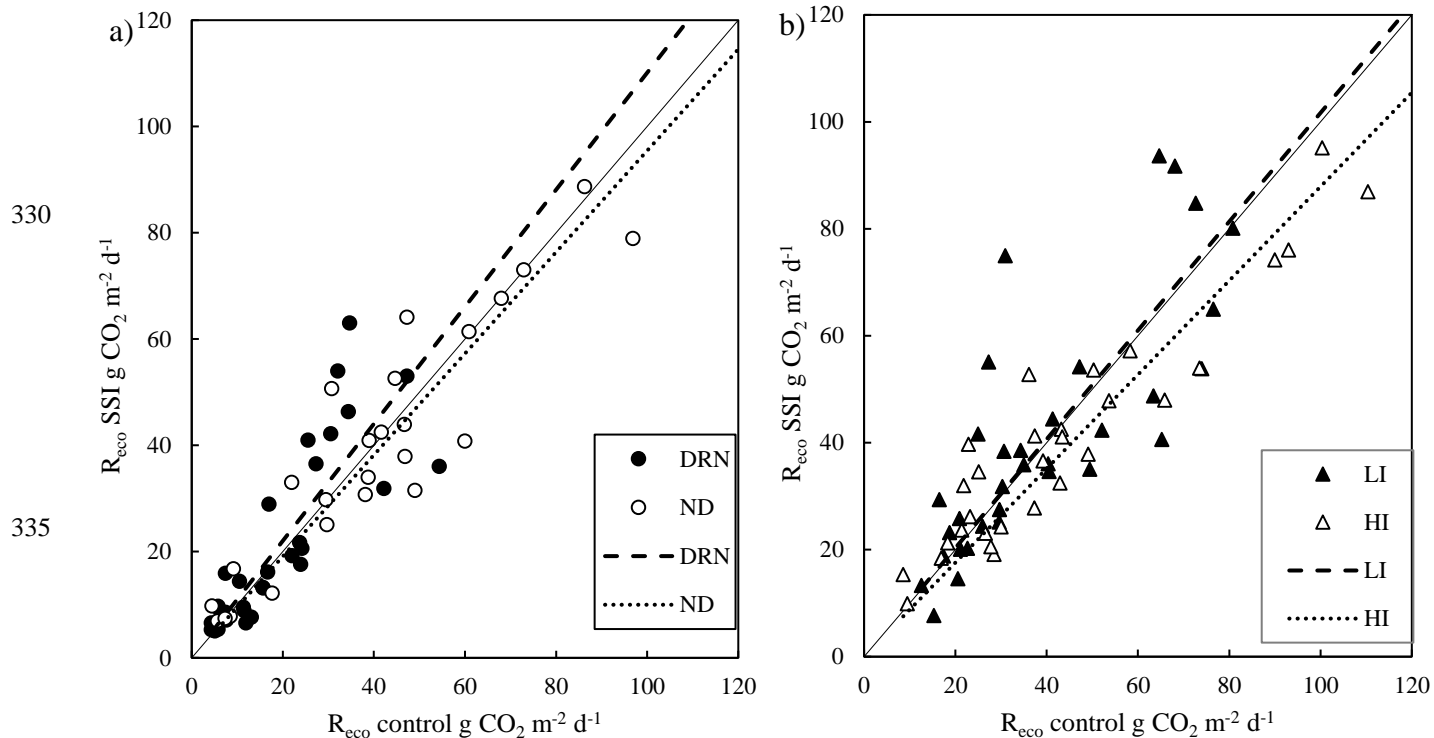
340

Figure 6 Measured fluxes for ecosystem respiration (R_{eco}), one-to-one comparison in which daily averages where used. a) Values divided into two groups: where the ground water table was lower due to the effect of drainage, and where there was a limited difference. B) Values divided into two groups with irrigation effects, moderate infiltration with more than 5–20 cm difference and high infiltration with more than 20cm difference between SSI and Control. Black filled line is the 1:1 line.

3.4 Annual carbon fluxes

3.4.1 Gross primary production (GPP)

345 GPP was high for all locations in both years, showing a clear seasonal pattern with the highest uptake at the start of the summer

(Fig.7). GPP was 30% lower in the dry year 2018 (p < 0.001) compared to 2017 (see Table 2) and differed between locations

(random effect p = 0.006). There was, however, no treatment effect on GPP (p = 0.3101). Average GPP values for all SSI and

control plots were -88.3±7.5 and -89.2±13 t CO_2 ha^{-1} yr^{-1} for 2017, -71.7±6.6 and -65.7±4.9 t CO_2 ha^{-1} yr^{-1} for 2018,

respectively.

3.4.2 Ecosystem respiration (R_{eco})

R_{eco} was generally high for all the farms measured during the two years, with the average R_{eco} of 128.4±4.6 t CO_2 ha^{-1} yr^{-1} for 2017 being significantly higher than100.8±11 t CO_2 ha^{-1} yr^{-1} for 2018 (p < 0.001) (Table 2). Different seasonal patterns were also observed between the two years, where in 2017 R_{eco} peaked in June and July, while in 2018 the highest R_{eco} was found in May (Fig. 7, Appendix B). However, no effect of SSI on R_{eco} was found (p = 0.6191), with average R_{eco} values for all SSI and control plots as 128.7±9.2 and 126.7±9.5 t CO_2 ha^{-1} yr^{-1} in 2017, 102.1±14.1 and 99.6±13.5 t CO_2 ha^{-1} yr^{-1} in 2018.

3.4.3 Net ecosystem exchange (NEE)

All locations functioned as large C sources during the measurement period. The average annual NEE of all sites amounted to 39.7±11 and 31.8±8.4 t CO_2 ha^{-1} yr^{-1} in 2017 and 2018, respectively. The overall explanatory power of year, treatment and location was low, with no yearly difference between 2017 and 2018 (p = 0.1813), or any treatment effect of SSI (p = 0.9805). The average NEE values for all SSI and control plots are 40.4±11.9 and 37.5±16.1 t CO_2 ha^{-1} yr^{-1} in 2017, 30.4±15.6 and 34±14.5 t CO_2 ha^{-1} yr^{-1} in 2018, respectively. or.

3.4.4 C-export (yield)

C-exports (i.e. yields) differed between years without treatment effect of SSI (p = 0.691). Following the drought in 2018, C export (13.8±0.6 t CO_2 ha^{-1} yr^{-1}) was significantly lower (p < 0.001) than in 2017 (18.0±1.4 t CO_2 ha^{-1} yr^{-1}). These values corresponded to dry matter yields of 9.4±0.6 t DM ha^{-1} yr-1 in 2018 and 12.6±1.1 t DM ha^{-1} yr-1 in 2017. The year-effect differed per location (random effect p < 0.001). We found a solid relationship between C-export and GPP (p < 0.001, r^2 = 0.942; linear-mixed modeling).

3.4.5 Net ecosystem carbon balance (NECB)

All sites are large carbon sources, without an effect of SSI (p = 0.9446) which was consistent for all farms (Table 3). However, there was a significant difference between the two years, with higher carbon emission rates in 2017 amounting to 49.6±11 t CO_2 eq. ha^{-1} yr^{-1} on average, compared with 36.9±7.6 t CO_2 eq. ha^{-1} yr^{-1} for 2018 (p=0.0277).

3.5 Methane exchange

The total exchange of CH_4 was very low during both years with no effect from the SSI (p=0.1147) or difference between years (p=0.1253). During most periods, the locations functioned as a sink of CH_4. The annual fluxes were -0.01 ± 0.01 t CO_2 eq. ha^{-1} yr^{-1} (-0.25 kg CH_4 ha^{-1} yr^{-1}) for 2017 and -0.06 ± 0.05 t CO_2 eq. ha^{-1} yr^{-1} (-1.8 kg CH_4 ha^{-1} yr^{-1}) for 2018 (Table 4). Such exchange did not play a significant part in the total GHG emissions (comparable to less than 0.4% of the annual NECB).

3.6 Nitrous oxide exchange

There was no treatment effect (p=0.5640) or inter-annual difference (p=0.4414) detected. The highest average emissions were measured on the SSI plot of location D, with 5.78 ± 5.9 mg N_2O. m^{-2} d^{-1} for 2017 and 10.7 ± 17.4 mg N_2O. m^{-2} d^{-1} for 2018. The highest peak was measured on the frame closest to the irrigation pipe in August for SSI of location D, showing 55 ± 15 mg N_2O m^{-2} d^{-1}. The peaks observed were erratic and did not correspond to fertilization management with slurry before measurement campaigns.

Table 3 Overview of all processes contributing to the carbon balance calculated for both years. Ecosystems respiration (R_{eco}), gross primary production (GPP), net ecosystems exchange (NEE, sum of GPP and R_{eco}), C-exports (harvest), C-manure (carbon addition from manure application), and net ecosystem carbon balance (NECB, sum of all fluxes) for subsoil irrigation (SSI) and control plots at farm locations A-D. The range of R_{eco}, GPP and NEE represent the combination of model error and extrapolation uncertainties following the law of error propagation.

			Carbon exchange					NECB
Year	Location	treatment	R_{eco}	GPP	NEE	C-export	C-manure	CO_2
			t CO_2 ha^{-1} yr^{-1}	t CO_2 ha^{-1} yr^{-1}	t CO_2 ha^{-1} yr^{-1}	t CO_2 ha^{-1} yr^{-1}	t CO_2 ha^{-1} yr^{-1}	t CO_2 ha^{-1} yr^{-1}
2017	A	SSI	123.1±3.4	-88.9±2.7	34.2±4.4	16.6	-6.9	46.8
		Control	133.7±6.5	-81.3±7.9	52.4±10.2	19.3	-6.9	65.7
	B	SSI	125±5.8	-98.5±3	26.5±6.5	15.3	-5.3	37.4
		Control	123.2±5.8	-92.6±2.9	30.6±6.5	15.5	-5.3	41.4
	C	SSI	132.1±4.6	-87.7±5.7	44.5±7.4	22.1	-10.9	55.8
		Control	122.3±3.2	-100±8.3	22.3±8.9	23.3	-10.9	35
	D	SSI	134.5±4.2	-78.6±2.8	56±5	15.7	-9.3	62.4
		Control	127.9±2	-82.9±5.3	44.9±5.6	16.3	-9.3	52.2
2018	A	SSI	98.3±6.5	-74.7±2.5	23.6±7	14	-7.4	29.7
		Control	101.3±5.5	-68.9±3.1	32.4±6.4	14	-7.4	38.5
	B	SSI	117.5±10.1	-73.4±3.4	44.2±10.7	13.8	-9.3	48.8
		Control	111.4±10.5	-64.5±2.8	46.9±10.9	12.2	-9.3	49.8
	C	SSI	109.6±5.8	-82.4±4.6	27.3±7.4	15.7	-9.3	32.6
		Control	99.2±1.3	-73.7±0.6	25.5±1.5	15.8	-9.3	31.5
	D	SSI	82.9±4.5	-56.1±2.2	26.8±5	13.4	-9.3	31
		Control	86.6±6.3	-55.5±2.4	31.1±7	12	-9.3	33.3

Table 4 The average measured CH$_4$ and N$_2$O emissions subsoil irrigation (SSI) and controls for the four locations (A-D) for both years in mg m^{-2} d^{-1}. The total CH$_4$ balance in CO$_2$ equivalents, using radiative forcing factors of 34 for CH$_4$ according to IPCC standards (Myhre et al., 2013). The ranges of CH$_4$ and N$_2$O represent the standard deviation (SD) of the measured fluxes.

			GHG fluxes		Balance
Year	Location	treatment	CH$_4$	N$_2$O	CH$_4$
			mg CH$_4$ m^{-2} d^{-1}	mg N$_2$O m^{-2} d^{-1}	t CO$_2$ eq. ha^{-1} yr^{-1}
2017	A	SSI	-0.44±0.5	0.02±0.7	-0.01
		Control	-0.54±0.9	1.46±1.8	-0.05
	B	SSI	-0.43±0.4	3.81±3.3	-0.04
		Control	-0.27±0.9	2.30±4.9	-0.02
	C	SSI	-0.43±1.0	2.48±1.5	-0.03
		Control	-0.40±0.5	2.56±2.0	0.01
	D	SSI	-0.50±0.8	5.78±5.9	0.01
		Control	0.72±2.7	4.81±2.3	0.06
2018	A	SSI	-0.39±0.7	0.15±0.8	-0.05
		Control	-0.67±1.2	0.80±0.9	-0.12
	B	SSI	-0.40±0.3	2.08±3.7	-0.04
		Control	-0.30±0.9	4.88±3.9	0.00
	C	SSI	-0.73±0.9	3.27±3.0	-0.11
		Control	-0.66±0.9	4.46±3.7	-0.07
	D	SSI	-0.91±0.6	10.7±17.4	-0.09
		Control	-0.14±0.8	2.69±2.2	0.02

395
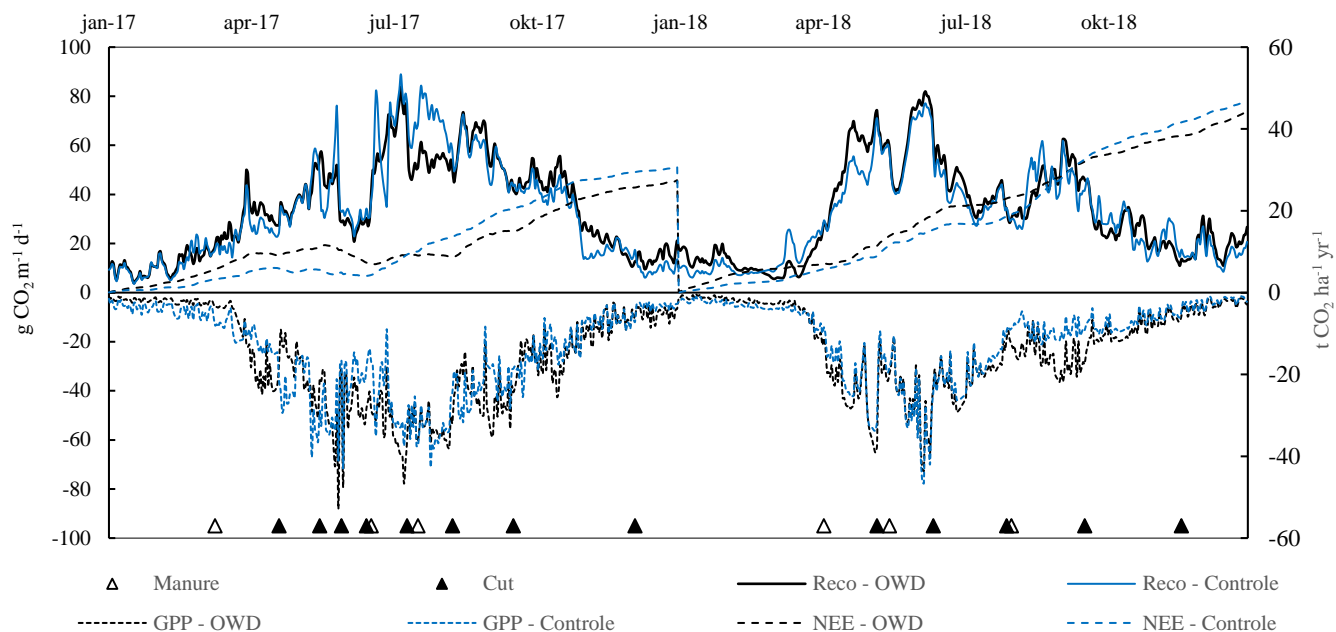
Figure 7 R_{eco} and GPP for location B in g CO_2 m^{-2} d^{-1} on the primary y-axis, for control and SSI. Accumulative NEE in t CO_2 ha^{-1} yr^{-1}, for control and subsoil irrigation (SSI), every year starting at 0.

4 Discussion

For both years, SSI had a clear irrigation effect during summer, increasing the averages of GWT during summer period by 6–18 cm at the four farms. During winter, there was a moderate but consistent drainage effect, reducing the average GWT in the wet/winter period by 1–20 cm. Despite the irrigation effects and higher water levels in summer, there was no effect of SSI on R_{eco} and total GHG balances remained high (62 t CO_2 eq. ha^{-1} yr^{-1} on average of all sites and years with an uncertainty of 3–16 t CO_2 ha^{-1} yr^{-1}). We found no evidence for a reduction of CO_2 emissions, nor for higher yields, on an annual base by implementing SSI.

4.1 SSI does not reduce annual R_{eco}

Based on the direct comparison using measured R_{eco} fluxes (Fig. 6), we found a modest 5–10% reduction in R_{eco} only when GWT differences were larger than 20 cm. When the irrigation effect was smaller, no effect on the R_{eco} was found. An earlier

study in the Netherlands on the role of GWT also showed small effects of higher summer GWT on R_{eco} and NEE despite substantial differences in soil volume changes/soil subsidence (Dirks et al., 2000). Similarly, a 4-year study (Schrier-Uijl et al., 2014) found little differences in NEE estimates despite substantial large variations in summer GWT and soil moisture contents.

Our findings contradict the general assumption that a higher GWT leads to lower CO_2 emissions, which is often found in near-natural peatlands with the presence of peat-forming vegetation (Moore and Dalva, 1993;Lloyd, 2006;Wilson et al., 2016). However, most studies discuss the effect of annual average GWT, instead of seasonal changes in GWT. In addition, there are also studies that did not find an effect of GWT on CO_2 emissions during the season (Lafleur et al., 2005;Nieveen et al., 2005;Parmentier et al., 2009). This lack of effect is explained by the fact that there is only a small variation in soil moisture values above the GWT. A large number of studies report lower CO_2 emissions when water levels were structurally elevated, concomitant with substantial differences in vegetation/land use following higher water levels (Beetz et al., 2013;Schrier-Uijl et al., 2014;Wilson et al., 2016). In our study, SSI seems to have an effect of a similar magnitude trending towards higher emissions during periods with lower GWT at the SSI sites.

The small effect size in our study can most probably be explained by differences in peat oxidation rates along the soil profile. Some other studies suggest that the top 30–40 cm layer of the peat profile plays an important role in C turnover rates in drained peatlands, due to more readily decomposable C sources and higher temperatures (Moore and Dalva, 1993;Lafleur et al., 2005;Karki et al., 2016;Saeurich et al., 2019). This soil layer was, however, not affected by higher summer GWTs in our study. Moreover, the topsoil layer was even exposed to oxygen for longer periods due to extra drainage during wet seasons. As the infiltrating water will affect the soil moisture content of these layers, it is even expected that this content will approach the optimum for C mineralization more often at the locations where SSI is applied. Saeurich et al. (2019) speculated that the highest CO_2 production in the top 10 cm is reached when GWTs are approximately 40 cm below the surface (Silvola et al., 1996).

In contrast to surface irrigation, where the topsoil is replenished with moisture, the SSI effect is limited to deeper parts of the peat soils, at -60--100 cm depth. However, the role of this deeper layer as a C source is only limited. Its potency to act as a C

440   source is reduced by lower temperatures, limited O_2 intrusion, and the fact that water content of this layer is already close to saturation (Berglund and Berglund, 2011;Taggart et al., 2012;Saeurich et al., 2019). This layer shows low levels of stronger electron acceptors such as O_2 and nitrate used for the microbial oxidation of organic compounds, and of labile organic matter (Fontaine et al., 2007;Leifeld et al., 2012). Visually, the layers deeper than 60 cm are less decomposed (plant macrofossils still visible) compared to the highly degraded uppermost 40 cm.

445

In addition, lower CO_2 production in deeper peat layers that are saturated due to the higher water level may be compensated by the increased CO_2 production in the top 20–40 cm due to the higher moisture levels resulting from elevated water levels. The dry year of 2018 with very low GWT in the control sites (and thus an expected maximized effect of SSI) provides additional evidence that SSI contributes little if any to the mitigation of CO_2 emission from drained peatlands. Such

450   understanding of the processes of CO_2 emissions in relation to soil profiles, along with the assumption from the Dutch soil-carbon-water model that the average lowest summer GWT is the major control of CO_2 emissions, is currently under investigation (STOWA, 2020)

4.2 SSI effects on CH_4 and N_2O emissions

The magnitudes of measured CH_4 and N_2O fluxes are substantially lower than CO_2, which would thus lead to negligible

455   contributions to the total GHG emissions in our case. Looking directly at the measured fluxes, no SSI effect was detected for neither CH_4 or N_2O. Findings of this experiment agree with the generally accepted idea that intensively drained peatlands have low levels of CH_4 emissions, and often these systems even function as a small CH_4 sink (Couwenberg et al., 2011;Couwenberg and Fritz, 2012;Tiemeyer et al., 2016;Maljanen et al., 2010). The SSI site in farm D showed the highest N_2O emissions with 10.7 ± 17.4 mg N_2O m^{-2} d^{-1} for 2017. In the current study the average measured N_2O emission was 12 kg

460   N_2O ha^{-1} yr^{-1} falling with the range of annual N_2O emissions from drained peatlands in Northern Europe (4-18 kg N_2O ha^{-1}) (Kandel et al., 2018;Leahy et al., 2004;Maljanen et al., 2010). Fertilization, temperature and water table fluctuations play

major roles in the total N_2O emission (Regina et al., 1999;Van Beek et al., 2011). No distinct peaks were measured after application of fertilizer, and fertilizer was applied on all locations on the same day, so missing peak fluxes would not influence the comparison. The mechanisms of N_2O production and consumption in organic soils are, however, complex and there is high temporal and spatial variability as influenced by site conditions and management (Leppelt et al., 2014;Taghizadeh-Toosi et al., 2019). Because of the low measurement interval for both years in the winter period, there is high chance of an underestimation of the N_2O emission, although this would not result in noticeable changes on the total GHG emissions. It is well studied that periods with frost and thawing result in high N_2O emissions (Koponen and Martikainen, 2004).

4.3 Reasonably high NEE

In contrast to the expected function of the SSI technique based on land subsidence data, no effect has been found on either promoting the yield/GPP nor reduction on NEE and other GHG emissions. Our NEE estimates from all sites and years at 35.8 (22.6 – 56.0) t CO_2 ha^{-1} yr^{-1} has exceeded the ranges reported for drained temperate peatlands, where Tiemeyer et al. (2020) reported 30.4 (5.1 – 40.3) t CO_2 ha^{-1} yr^{-1} for the German drained organic soils, and Veenendaal et al. (2007) reported 4.9 t CO_2 ha^{-1} yr^{-1} in an earlier analysis at an intensively managed Dutch peat meadow measured with eddy covariance. Looking into GPP and R_{eco} individually, on the one hand, the GPP of the sites was higher than values found by Tiemeyer et al. (2016) for productive and drained peatlands (-70 ± 18 t CO_2 ha^{-1} yr^{-1}) especially in the year 2017 (-88.7±7.2 t CO_2 ha^{-1} yr^{-1}), and falls back to the range in 2018 (-69.0±8.9 t CO_2 ha^{-1} yr^{-1}) due to the drought induced decline of CO_2 uptake (Fu et al., 2020). This could be simply explained by the high productivity of the sites, where the C-export in 2017 (on average 18.0 t CO_2 ha^{-1}) was substantially larger than the 8.5 t CO_2 ha^{-1} reported by Tiemeyer et al. (2016) for grassland on organic soils. On the other hand, the R_{eco} values of the sites (128.4±4.6 and 100.8±11 t CO_2 ha^{-1} yr^{-1} in 2017 and 2018, respectively) are also at the higher end of the range (97 ± 33 t CO_2 ha^{-1} yr^{-1} in Tiemeyer et al. (2016)). Extrapolation bias was excluded as a possible reason for this high CO_2 emission, since testing of different R_{eco} modeling approaches (including different model selection, data clustering procedure and removal of raw data outliers) did not yield substantially difference R_{eco} values (Järveoja et al., 2020) discovered in a boreal natural peatland strong diel patterns of R_{eco} with peaks at both midnight and midday, which could lead to

overestimation of daily fluxes when models are developed with data collected around the peaks. Although this process is not clear for temperate productive peatland systems, representativeness of the campaign could be a reason for the high R_{eco} estimates. Besides the methodological speculations, there are also a number of biochemical reasons for the high emissions found here. Abiotic conditions that favor high CO_2 emissions were present, with high temperatures for both years and non-limiting moisture conditions for 2017. Research from (Pohl et al., 2015) found a high impact of dynamic soil organic carbon (SOC) and N stocks in the aerobic zone on CO_2 fluxes. In our case, the peat soils contained a high amount of C, especially in the upper 20 cm layer. This layer was also aerobic for long periods during the experiment, thus promoting C formation and transformation processes in the plant–soil system.

4.4 Uncertainties

GHG emissions on peat grasslands are highly variable (Tiemeyer et al., 2016) given the uncertainties from the wide ranges of land use and management activities (Renou-Wilson et al., 2016) and gap filling techniques (Huth et al., 2017). In this study, besides the model errors inherent in the model development process, uncertainties from gap-filling techniques in terms of data-pooling strategies and model selections were also considered. Campaign-wise fitting of R_{eco} and GPP models can best represent the original data sets, while pooling data for a longer period can provide better model fitness and less bias toward single measurements (Huth et al., 2017;Poyda et al., 2017). However, in this study, different responses of vegetation and soil processes to drought, especially to the extreme drought in 2018, caused data points that could not be represented by the classic models, resulting in the generally poor performances of annual models. For this reason, we reported the annual budgets with campaign-wise gap-filled NEE values. The uncertainties of NEE estimates from model differences were on average 14 tons and up to 25 tons of CO_2. Nevertheless, no SSI effect was found considering NEE estimates from annual models. The model differences quantified here were in good agreements with other model tests (Görres et al., 2014;Karki et al., 2019) and match the magnitude of NEE uncertainties calculated with other methods (e.g. the 23–30 tons CO2 variances reported by (Schrier-Uijl et al., 2014) using eddy co-variance techniques).

4.5 Costs and benefits of the SSI

The intensity of land use (intensity and timing of drainage and fertilization, plant species composition, mowing and grazing regimes) influence the grassland's ability to accumulate or lose C (Renou-Wilson et al., 2016;Smith, 2014;Ward et al., 2016). SSI can increase the load-bearing capacity of the field surface for fertilizing equipment, facilitating earlier fertilization compared to management under current drainage systems. This can also cause increased leaching of water due to earlier drainage in a wet spring. However, the general land-use intensity will not change with the use of SSI. It was expected that C-export via crop yields due to extra drainage could increase in a wet autumn. However, we did not find any indication for an increase in land-use intensity or yield as a result of SSI.

The use of SSI is considered impractical for use in most regions outside of the Netherlands due to the high investment costs for irrigation pipes and the intensive water infrastructure needed for controlling the water level. In addition, irrigation pipes will increase the water demand in summer for these agricultural fields. Both land-use intensity and an increase in yield are related to an increase in CO_2 emissions on drained peat (Couwenberg, 2011;Beetz et al., 2013). The land-use history of our sites favors high CO_2 emission: tillage (cultivators, sod-renewal, and some plowing), cumulative fertilization and well-maintained drainage (Provincie Fryslân ,2015).

5 Main conclusions

The implementation of SSI technique with the current design does not lead to a reduction of GHG emissions from drained peat meadows, even though there was a clear increase in GWT during summer (especially in the dry year of 2018). We therefore conclude that the current use of SSI with the aim to raise the water table to -60 cm is ineffective as a mitigation measure to sufficiently lower peat oxidation rates and, therefore, also soil subsidence. Most likely, the largest part of the peat oxidation takes place in the top 70 cm of the soil, which stays above the GWT with the use of SSI. This layer is still exposed to higher temperatures, sufficient moisture, oxygen and alternative electron acceptors such as nitrate, and nutrient input. We expect that

530 SSI may only be effective when the GWT can be raised permanently to levels close to the soil surface (20–35 cm below the surface).

Data availability. The data are available on request from the corresponding author, (S.T.J. Weideveld).

535 **CRediT authorship contribution statement:**

SW: Investigation, Data curation, Writing – original draft, Visualization, Methodology. WL: Investigation, Data curation, Writing – original draft, Visualization. MB: Data curation, Writing – original draft, Visualization. LL: Writing - review & editing, Supervision.CZ: Conceptualization, Methodology, Writing - original draft, Supervision

Acknowledgements

540 We would like to thank all technical staff, students and others who helped in the field and in the laboratory, as well as the land owners who granted access to the measurement sites. We acknowledge Peter Cruijsen and Roy Peters for their assistance in practical work and analyses. Weier Liu is supported by the China Scholarship Council.

Appendix A Annual models

545   Table A1. Model selected for annual-model gap-filling approach of year budgets (adopted from Karki et al. 2019), as a measure of extrapolation uncertianties.

Model		Structure	Description
R_eco	1	$Reco_{Tref} * e^{E_0 * \left(\frac{1}{T_{ref} - T_0} - \frac{1}{T - T_0} \right)}$	Arrhenius function used for the campaign-wise model fit. Parameters follow descriptions in Material and Methods.
	2	$(Reco_{Tref} + (\alpha * GH)) * e^{E_0 * \left(\frac{1}{T_{ref} - T_0} - \frac{1}{T - T_0} \right)}$	Model 1 adding GH (grass height) as a vegetation factor. α is a scaling parameter of GH.
	3	$Reco_{Tref} * e^{E_0 * \left(\frac{1}{T_{ref} - T_0} - \frac{1}{T - T_0} \right)} + (\alpha * GH)$	Different form of vegetation included Model 1.
	4	$R_0 * e^{bT}$	Exponential function. R_0 is respiration at 0 °C, b is a temperature sensitivity parameter.
	5	$(R_0 + (\alpha * GH)) * e^{bT}$	Model 4 with vegetation included.
	6	$R_0 + (b * T) + (\alpha * GH)$	Linear function.
GPP	1	$\dfrac{\alpha * PAR * GPP_{max}}{GPP_{max} + \alpha * PAR}$	Michaelis-Menten light response curve as used for the campaign-wise model fitting.
	2	$\dfrac{\alpha * PAR * GPP_{max} * GH}{GPP_{max} * GH + \alpha * PAR} * FT$	Model 1 with vegetation and air temperature included. FT is a temperature dependent function of photosynthesis set to 0 below - 2 °C and 1 above 10 °C and

			with an exponential increase between - 2 and 10 °C.
	3	$$\frac{GPP_{max} * PAR}{\kappa + PAR} * (\frac{GH}{GH + a})$$	Another form of the Michaelis-Menten light response curve with a vegetation term included. a is a model-specific parameter.
	4	$$\frac{GPP_{max} * PAR}{\kappa + PAR} * (\frac{GH}{GH + a}) * FT$$	Model 3 with air temperature included.

Appendix B – Soil type decryption

Table B1 Soil characteristics of the research sites in Frisian peat meadows. Average per soil type, gravimetric soil moisture content taken August 2017, Dry bulk density, Organic matter content, and elemental Carbon content.

Farm	Treatment	Soil type	Depth	Soil moisture %	Bulk density g DW/cm3	Organic matter g Org/L	Carbon content g C/L
A	SSI	Mineral	0-35	38.1	0.99	122.6	52.3
		Peat	35-60	77.1	0.23	144.0	77.1
		Peat	60-80	82.1	0.14	130.4	67.9
	Control	Mineral	0-40	37.6	0.93	130.1	53.6
		Peat	40-60	59.2	0.24	156.0	82.9
		Peat	60-80	85.3	0.16	153.8	98.1
B	SSI	Peat	0-20	51.0	0.44	270.3	107.6
		Peat	20-60	79.3	0.19	168.9	76.6
		Peat	60-80	88.4	0.12	118.3	59.9
	Control	Peat	0-20	50.1	0.49	273.4	138.3
		Peat	20-60	77.7	0.17	140.6	72.0
		Peat	60-80	86.5	0.13	122.0	66.9
C	SSI	Mineral	0-30	36.0	0.71	127.9	58.2
		Schalter	30-40	79.2	0.19	176.9	87.5
		Peat	40-60	82.2	0.18	128.5	64.2
		Peat	60-80	87.5	0.11	132.9	81.4
	Control	Mineral	0-30	38.0	0.75	141.7	59.2
		Schalter	30-40	78.7	0.19	176.9	92.4
		Peat	40-60	84.3	0.12	116.3	59.9
		Peat	60-80	89.2	0.10	133.6	71.5
D	SSI	Mineral	0-30	37.7	0.85	154.5	73.7
		Schalter	30-40	63.9	0.30	266.5	85.2
		Peat	40-60	84.3	0.19	137.0	73.1
		Peat	60-80	80.2	0.14	129.6	54.6
	Control	Mineral	0-25	32.9	0.82	140.7	73.3
		Schalter	25-35	70.0	0.27	172.6	85.9
		Peat	35-60	84.1	0.15	141.9	82.7
		Peat	60-80	81.9	0.11	108.5	69.5
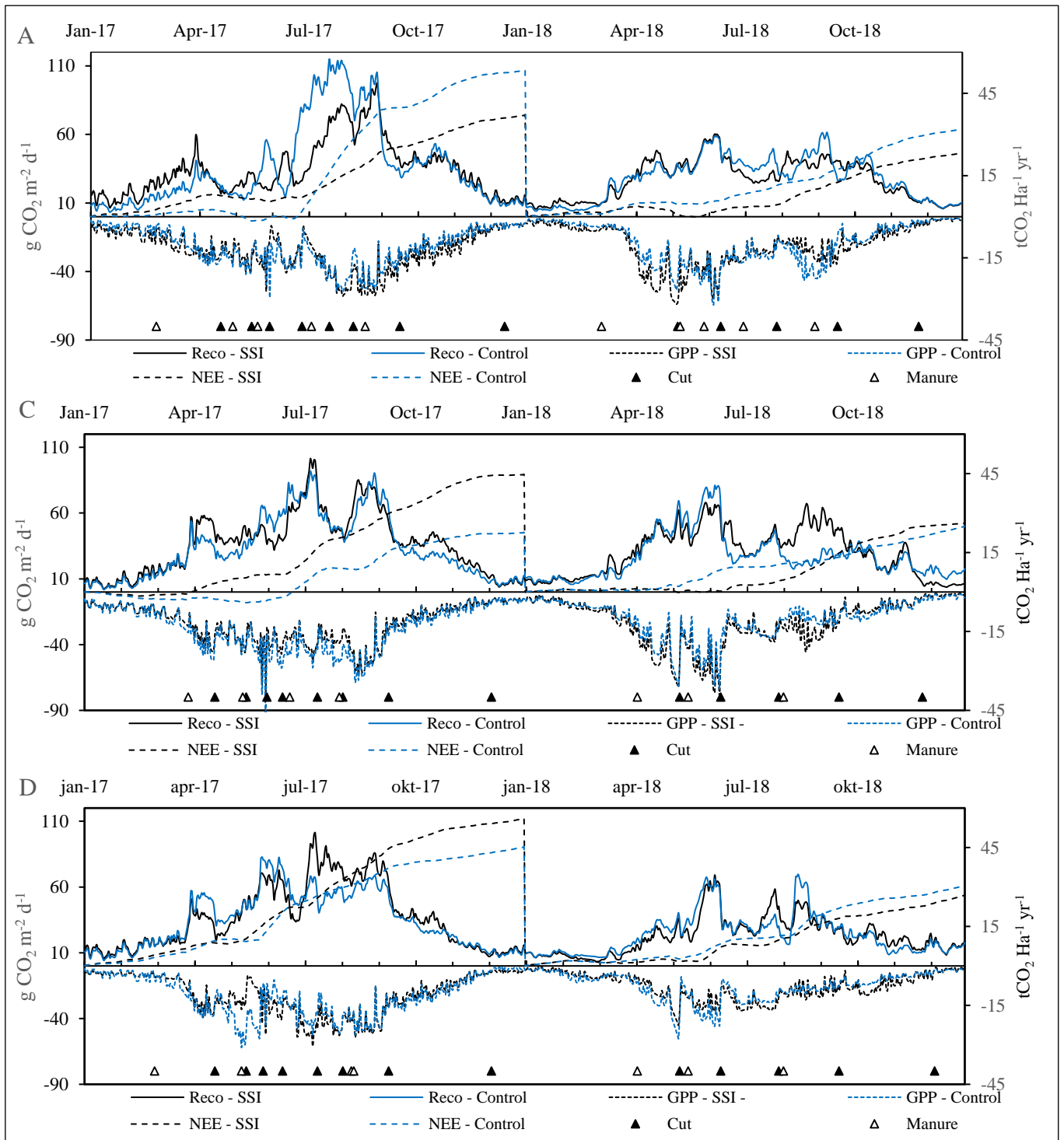
Figure C1 Daily R$_{eco}$ and GPP for location in g CO^2 m^{-1} d^{-1} on the primary y-axis, for control and SSI for locations A,C and D. Accumulative NEE in tCO^2 Ha^{-1} yr^{-1}, for control and SSI, every year starting at 0.

Appendix D CH4 exchange
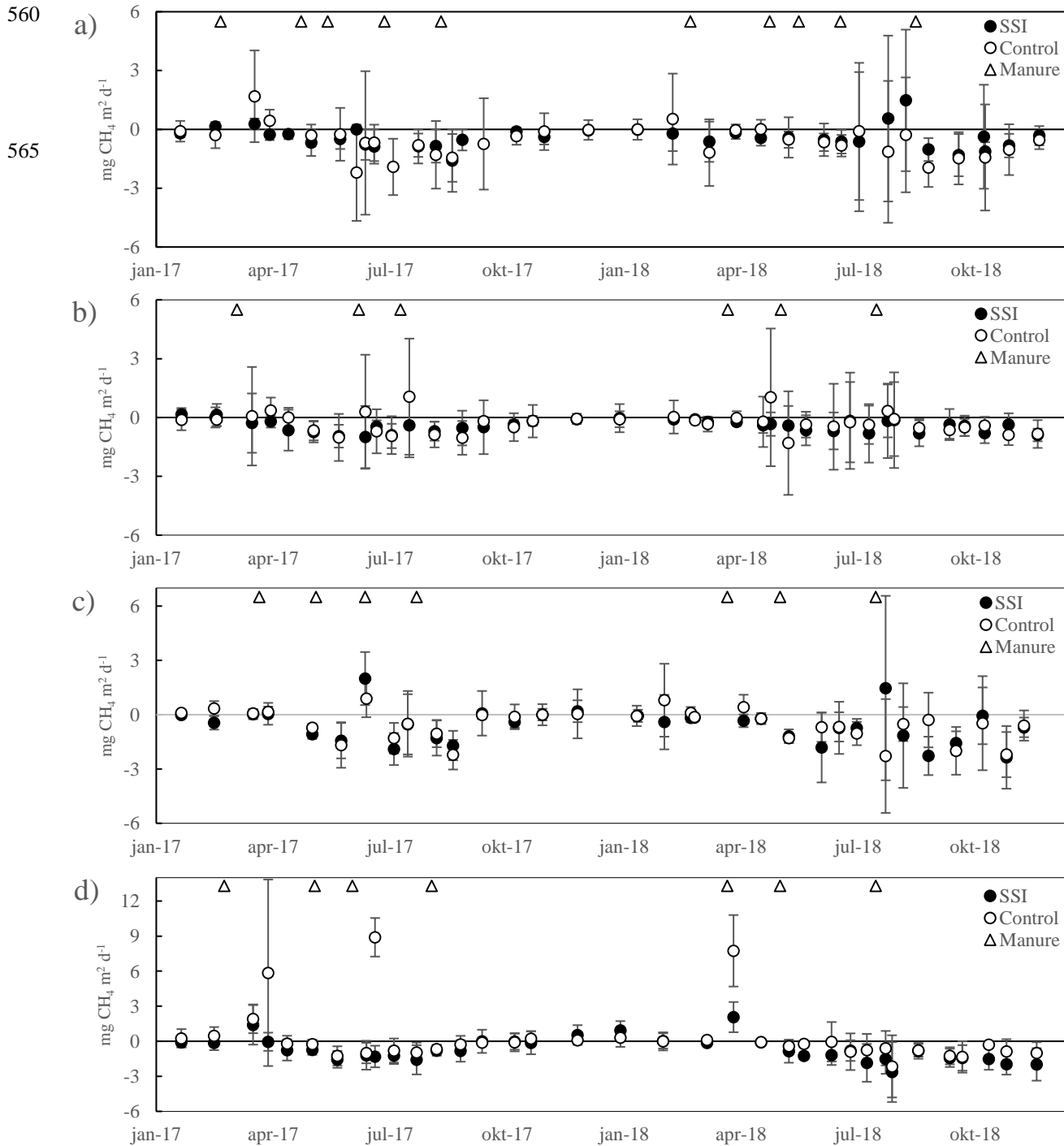
Figure D1 CH4 exchange throughout 2017 and 2018 in mg CH4 m-2 d-1

 Appendix E N₂O exchange
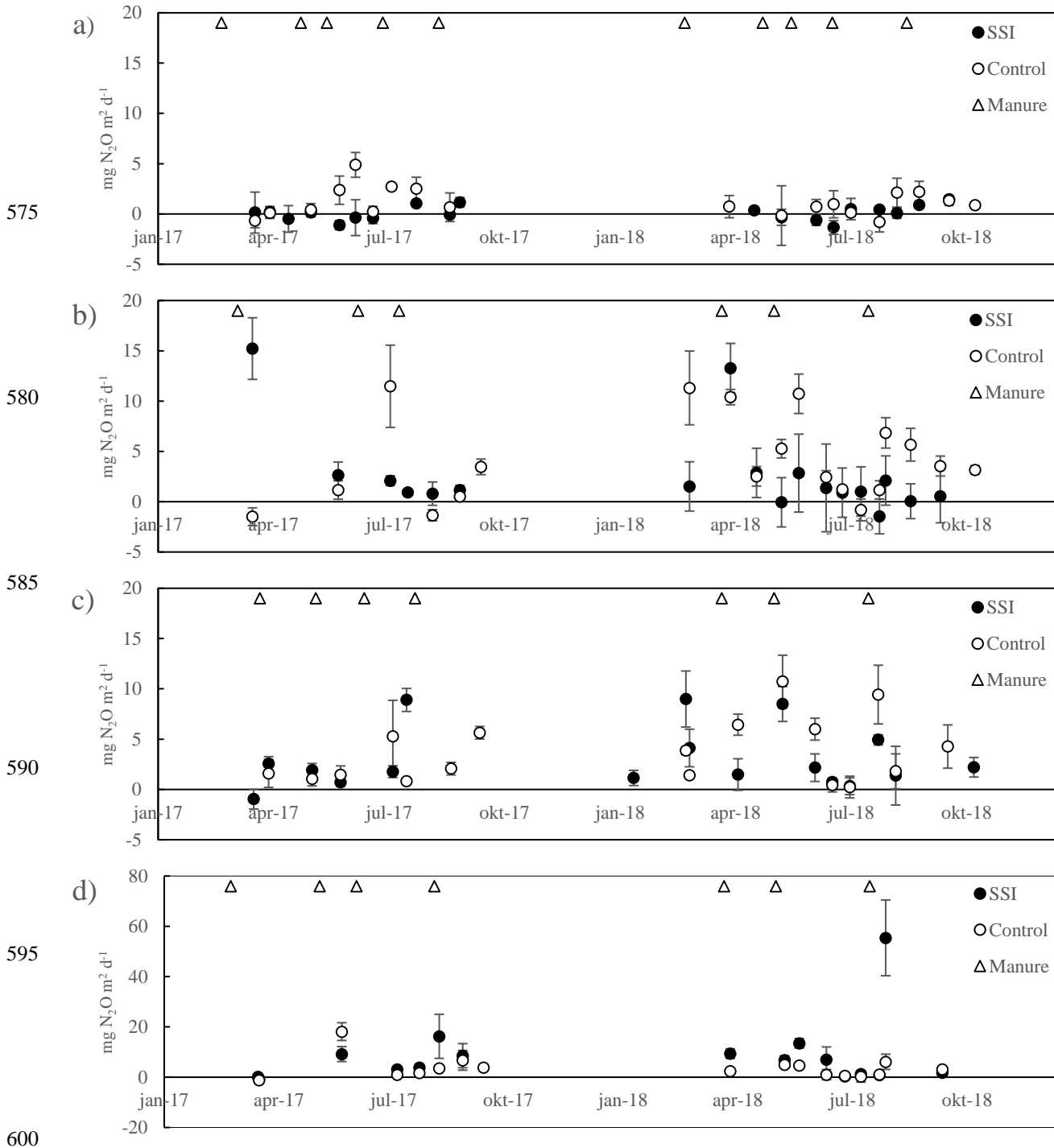
Figure E1 N₂O exchange throughout 2017 and 2018 in mg N₂O m⁻² d⁻¹.

References

Almeida, R. M., Nóbrega, G. N., Junger, P. C., Figueiredo, A. V., Andrade, A. S., de Moura, C. G., Tonetta, D., Oliveira Jr, E. S., Araújo, F., and Rust, F.: High primary production contrasts with intense carbon emission in a eutrophic tropical reservoir, Frontiers in microbiology, 7, 717, 2016.

605   Arets, E. J. M. M., Van Der Kolk, J., Hengeveld, G. M., Lesschen, J. P., Kramer, H., Kuikman, P., and Schelhaas, N.: Greenhouse gas reporting for the LULUCFsector in the Netherlands: methodological background, update 2020, Statutory Research Tasks Unit for Nature & the Environment2352-2739, 2020.

Bates, D., Mächler, M., Bolker, B., and Walker, S.: Fitting linear mixed-effects models using lme4, arXiv preprint arXiv:1406.5823, 2014.

610   Beetz, S., Liebersbach, H., Glatzel, S., Jurasinski, G., Buczko, U., and Höper, H.: Effects of land use intensity on the full greenhouse gas balance in an Atlantic peat bog, Biogeosciences, 10, 1067-1082, 2013.

Berglund, Ö., and Berglund, K.: Influence of water table level and soil properties on emissions of greenhouse gases from cultivated peat soil, Soil Biology and Biochemistry, 43, 923-931, 2011.

Brouns, K., Eikelboom, T., Jansen, P. C., Janssen, R., Kwakernaak, C., van den Akker, J. J., and Verhoeven, J. T.: Spatial
615   analysis of soil subsidence in peat meadow areas in Friesland in relation to land and water management, climate change, and adaptation, Environmental management, 55, 360-372, 2015.

Couwenberg, J.: Greenhouse gas emissions from managed peat soils: is the IPCC reporting guidance realistic?, Mires & Peat, 8, 2011.

Couwenberg, J., Thiele, A., Tanneberger, F., Augustin, J., Bärisch, S., Dubovik, D., Liashchynskaya, N., Michaelis, D., Minke,
620   M., and Skuratovich, A.: Assessing greenhouse gas emissions from peatlands using vegetation as a proxy, Hydrobiologia, 674, 67-89, 2011.

Couwenberg, J., and Fritz, C.: Towards developing IPCC methane 'emission factors' for peatlands (organic soils), Mires and Peat, 10, 1-17, 2012.

Dawson, Q., Kechavarzi, C., Leeds-Harrison, P., and Burton, R.: Subsidence and degradation of agricultural peatlands in the
625   Fenlands of Norfolk, UK, Geoderma, 154, 181-187, 2010.

Dirks, B., Hensen, A., and Goudriaan, J.: Effect of drainage on CO2 exchange patterns in an intensively managed peat pasture, Climate Research, 14, 57-63, 2000.

Erkens, G., van der Meulen, M. J., and Middelkoop, H.: Double trouble: subsidence and CO 2 respiration due to 1,000 years of Dutch coastal peatlands cultivation, Hydrogeology Journal, 24, 551-568, 2016.

630   Falge, E., Baldocchi, D., Olson, R., Anthoni, P., Aubinet, M., Bernhofer, C., Burba, G., Ceulemans, R., Clement, R., and Dolman, H.: Gap filling strategies for long term energy flux data sets, Agricultural and Forest Meteorology, 107, 71-77, 2001.

Fontaine, S., Barot, S., Barré, P., Bdioui, N., Mary, B., and Rumpel, C.: Stability of organic carbon in deep soil layers controlled by fresh carbon supply, Nature, 450, 277-280, 2007.

635 Fox, J., and Weisberg, S.: An R companion to applied regression, Sage Publications, 2018.

Fu, Z., Ciais, P., Bastos, A., Stoy, P. C., Yang, H., Green, J. K., Wang, B., Yu, K., Huang, Y., and Knohl, A.: Sensitivity of gross primary productivity to climatic drivers during the summer drought of 2018 in Europe, Philosophical Transactions of the Royal Society B, 375, 20190747, 2020.

Gorham, E., Lehman, C., Dyke, A., Clymo, D., and Janssens, J.: Long-term carbon sequestration in North American peatlands,
640 Quaternary Science Reviews, 58, 77-82, 2012.

Görres, C.-M., Kutzbach, L., and Elsgaard, L.: Comparative modeling of annual CO_2 flux of temperate peat soils under permanent grassland management, Agriculture, ecosystems & environment, 186, 64-76, 2014.

Hartman, A., Schouwenaars, J., and Moustafa, A.: De kosten voor het waterbeheer in het veenweidegebied van Friesland, H 2 O, 45, 25, 2012.

645 Heiri, O., Lotter, A. F., and Lemcke, G.: Loss on ignition as a method for estimating organic and carbonate content in sediments: reproducibility and comparability of results, Journal of paleolimnology, 25, 101-110, 2001.

Hendriks, R., Wollewinkel, R., and Van den Akker, J.: Predicting soil subsidence and greenhouse gas emission in peat soils depending on water management with the SWAP-ANIMO model, Proceedings of the First International Symposium on Carbon in Peatlands, Wageningen, The Netherlands, 15-18 April 2007, 2007, 583-586,

650 Herbert, E. R., Boon, P., Burgin, A. J., Neubauer, S. C., Franklin, R. B., Ardón, M., Hopfensperger, K. N., Lamers, L. P., and Gell, P.: A global perspective on wetland salinization: ecological consequences of a growing threat to freshwater wetlands, Ecosphere, 6, 1-43, 2015.

Hiraishi, T., Krug, T., Tanabe, K., Srivastava, N., Baasansuren, J., Fukuda, M., and Troxler, T.: 2013 supplement to the 2006 IPCC guidelines for national greenhouse gas inventories: Wetlands, IPCC, Switzerland, 2014.

655 Hoffmann, M., Jurisch, N., Borraz, E. A., Hagemann, U., Drösler, M., Sommer, M., and Augustin, J.: Automated modeling of ecosystem CO_2 fluxes based on periodic closed chamber measurements: A standardized conceptual and practical approach, Agricultural and forest meteorology, 200, 30-45, 2015.

Hoogland, T., Van den Akker, J., and Brus, D.: Modeling the subsidence of peat soils in the Dutch coastal area, Geoderma, 171, 92-97, 2012.

660 Hooijer, A., Page, S., Canadell, J., Silvius, M., Kwadijk, J., Wosten, H., and Jauhiainen, J.: Current and future CO_2 emissions from drained peatlands in Southeast Asia, Biogeosciences, 2010.

Hoving, I., Vereijken, P., van Houwelingen, K., and Pleijter, M.: Hydrologische en landbouwkundige effecten toepassing onderwaterdrains bij dynamisch slootpeilbeheer op veengrond, Wageningen UR Livestock Research, 2013.

Huth, V., Vaidya, S., Hoffmann, M., Jurisch, N., Günther, A., Gundlach, L., Hagemann, U., Elsgaard, L., and Augustin, J.:
665 Divergent NEE balances from manual-chamber CO_2 fluxes linked to different measurement and gap-filling

strategies: A source for uncertainty of estimated terrestrial C sources and sinks?, Journal of Plant Nutrition and Soil Science, 180, 302-315, 2017.

Järveoja, J., Nilsson, M. B., Crill, P. M., and Peichl, M.: Bimodal diel pattern in peatland ecosystem respiration rebuts uniform temperature response, Nature communications, 11, 1-9, 2020.

670   Joosten, H., and Clarke, D.: Wise use of mires and peatlands: background and principles including a framework for decision-making, International Mire Conservation Group, 2002.

Joosten, H.: The Global Peatland CO2 Picture: peatland status and drainage related emissions in all countries of the world, The Global Peatland CO2 Picture: peatland status and drainage related emissions in all countries of the world., 2009.

Jurasinski, G., Glatzel, S., Hahn, J., Koch, S., Koch, M., and Koebsch, F.: Turn on, fade out-methane exchange in a coastal 675   fen over a period of six years after rewetting, EGU General Assembly Conference Abstracts, 2016,

Kabat, P., Fresco, L. O., Stive, M. J., Veerman, C. P., Van Alphen, J. S., Parmet, B. W., Hazeleger, W., and Katsman, C. A.: Dutch coasts in transition, Nature Geoscience, 2, 450-452, 2009.

Kandel, T. P., Lærke, P. E., and Elsgaard, L.: Effect of chamber enclosure time on soil respiration flux: A comparison of linear and non-linear flux calculation methods, Atmospheric environment, 141, 245-254, 2016.

680   Kandel, T. P., Laerke, P. E., and Elsgaard, L.: Annual emissions of CO2, CH4 and N2O from a temperate peat bog: Comparison of an undrained and four drained sites under permanent grass and arable crop rotations with cereals and potato, Agricultural and Forest Meteorology, 256, 470-481, 2018.

Karki, S., Elsgaard, L., Kandel, T. P., and Lærke, P. E.: Carbon balance of rewetted and drained peat soils used for biomass production: a mesocosm study, Gcb Bioenergy, 8, 969-980, 2016.

685   Karki, S., Kandel, T., Elsgaard, L., Labouriau, R., and Lærke, P.: Annual CO 2 fluxes from a cultivated fen with perennial grasses during two initial years of rewetting, Mires & Peat, 25, 2019.

Koponen, H. T., and Martikainen, P. J.: Soil water content and freezing temperature affect freeze–thaw related N 2 O production in organic soil, Nutrient Cycling in Agroecosystems, 69, 213-219, 2004.

Kuikman, P., van den Akker, J., and de Vries, F.: Emission of N2O and CO2 from organic agricultural soils, Alterra report, 690   1035, 2005.

Kuznetsova, A., Brockhoff, P. B., and Christensen, R. H. B.: lmerTest package: tests in linear mixed effects models, Journal of Statistical Software, 82, 2017.

Lafleur, P., Moore, T. R., Roulet, N. T., and Frolking, S.: Ecosystem respiration in a cool temperate bog depends on peat temperature but not water table, Ecosystems, 8, 619-629, 2005.

695   Lamers, L. P., Vile, M. A., Grootjans, A. P., Acreman, M. C., van Diggelen, R., Evans, M. G., Richardson, C. J., Rochefort, L., Kooijman, A. M., and Roelofs, J. G.: Ecological restoration of rich fens in Europe and North America: from trial and error to an evidence-based approach, Biological Reviews, 90, 182-203, 2015.

Leahy, P., Kiely, G., and Scanlon, T. M.: Managed grasslands: A greenhouse gas sink or source?, Geophysical Research Letters, 31, 2004.

700 Leifeld, J., Steffens, M., and Galego-Sala, A.: Sensitivity of peatland carbon loss to organic matter quality, Geophysical Research Letters, 39, 2012.

Leifeld, J., and Menichetti, L.: The underappreciated potential of peatlands in global climate change mitigation strategies, Nature communications, 9, 1-7, 2018.

Leppelt, T., Dechow, R., Gebbert, S., Freibauer, A., and Lohila, A.: Nitrous oxide emission budgets and land-use-driven
705 hotspots for organic soils in Europe, Biogeosciences, 11, 6595-6612, 2014.

Lloyd, C.: Annual carbon balance of a managed wetland meadow in the Somerset Levels, UK, Agricultural and Forest Meteorology, 138, 168-179, 2006.

Lloyd, J., and Taylor, J.: On the temperature dependence of soil respiration, Functional ecology, 315-323, 1994.

Lüdecke, D.: sjstats: Statistical Functions for Regression Models (Version 0.17. 4). doi: 10.5281/zenodo. 1284472. 2019.

710 Maljanen, M., Sigurdsson, B., Guðmundsson, J., Óskarsson, H., Huttunen, J., and Martikainen, P.: Greenhouse gas balances of managed peatlands in the Nordic countries–present knowledge and gaps, Biogeosciences, 7, 2711-2738, 2010.

Moore, T., and Dalva, M.: The influence of temperature and water table position on carbon dioxide and methane emissions from laboratory columns of peatland soils, Journal of Soil Science, 44, 651-664, 1993.

Myhre, G., Shindell, D., Bréon, F., Collins, W., Fuglestvedt, J., Huang, J., Koch, D., Lamarque, J., Lee, D., and Mendoza, B.:
715 Anthropogenic and Natural Radiative Forcing, Climate Change 2013: The Physical Science Basis. Contribution of Working Group I to the Fifth Assessment Report of the Intergovernmental Panel on Climate Change, 659–740. Cambridge: Cambridge University Press, 2013.

Nieveen, J. P., Campbell, D. I., Schipper, L. A., and Blair, I. J.: Carbon exchange of grazed pasture on a drained peat soil, Global Change Biology, 11, 607-618, 2005.

720 Parmentier, F., Van der Molen, M., De Jeu, R., Hendriks, D., and Dolman, A.: CO2 fluxes and evaporation on a peatland in the Netherlands appear not affected by water table fluctuations, Agricultural and forest meteorology, 149, 1201-1208, 2009.

Pohl, M., Hoffmann, M., Hagemann, U., Giebels, M., Albiac Borraz, E., Sommer, M., and Augustin, J.: Dynamic C and N stocks--key factors controlling the C gas exchange of maize in heterogenous peatland, Biogeosciences, 12, 2015.

725 Poyda, A., Reinsch, T., Kluß, C., Loges, R., and Taube, F.: Greenhouse gas emissions from fen soils used for forage production in northern Germany, Biogeosciences, 13, 5221-5244, 2016.

Poyda, A., Reinsch, T., Skinner, R. H., Kluß, C., Loges, R., and Taube, F.: Comparing chamber and eddy covariance based net ecosystem CO2 exchange of fen soils, Journal of Plant Nutrition and Soil Science, 180, 252-266, 2017.

Querner, E., Jansen, P., Van Den AKKER, J., and Kwakernaak, C.: Analysing water level strategies to reduce soil subsidence
730 in Dutch peat meadows, Journal of hydrology, 446, 59-69, 2012.

Regina, K., Silvola, J., and Martikainen, P. J.: Short-term effects of changing water table on N2O fluxes from peat monoliths from natural and drained boreal peatlands, Global Change Biology, 5, 183-189, 1999.

Regina, K., Syväsalo, E., Hannukkala, A., and Esala, M.: Fluxes of N2O from farmed peat soils in Finland, European Journal of Soil Science, 55, 591-599, 2004.

735 Regina, K.: Greenhouse gas emissions of cultivated peatlands and their mitigation, Suo, 65, 21-23, 2014.

Renou-Wilson, F., Müller, C., Moser, G., and Wilson, D.: To graze or not to graze? Four years greenhouse gas balances and vegetation composition from a drained and a rewetted organic soil under grassland, Agriculture, Ecosystems & Environment, 222, 156-170, 2016.

Saeurich, A., Tiemeyer, B., Dettmann, U., and Don, A.: How do sand addition, soil moisture and nutrient status influence
740 greenhouse gas fluxes from drained organic soils?, Soil Biology and Biochemistry, 135, 71-84, 2019.

Schrier-Uijl, A., Kroon, P., Hendriks, D., Hensen, A., Van Huissteden, J., Berendse, F., and Veenendaal, E.: Agricultural peatlands: towards a greenhouse gas sink-a synthesis of a Dutch landscape study, Biogeosciences, 11, 4559, 2014.

Silvola, J., Alm, J., Ahlholm, U., Nykanen, H., and Martikainen, P. J.: CO_2 fluxes from peat in boreal mires under varying temperature and moisture conditions, Journal of ecology, 219-228, 1996.

745 Smith, P.: Do grasslands act as a perpetual sink for carbon?, Global change biology, 20, 2708-2711, 2014.

Stephens, J. C., Allen Jr, L., and Chen, E.: Organic soil subsidence, Reviews in Engineering Geology, 6, 107-122, 1984.

STOWA: Nationaal onderzoeksprogramma broeikasgassen veenweide: Eb en vloed in de polder. In: STOWA Ter info, 2020.

Syvitski, J. P., Kettner, A. J., Overeem, I., Hutton, E. W., Hannon, M. T., Brakenridge, G. R., Day, J., Vörösmarty, C., Saito, Y., and Giosan, L.: Sinking deltas due to human activities, Nature Geoscience, 2, 681, 2009.

750 Taggart, M., Heitman, J. L., Shi, W., and Vepraskas, M.: Temperature and Water Content Effects on Carbon Mineralization for Sapric Soil Material, Wetlands, 32, 939-944, 2012.

Taghizadeh-Toosi, A., Clough, T., Petersen, S. O., and Elsgaard, L.: Nitrous Oxide Dynamics in Agricultural Peat Soil in Response to Availability of Nitrate, Nitrite, and Iron Sulfides, Geomicrobiology Journal, 1-10, 10.1080/01490451.2019.1666192, 2019.

755 Tanneberger, F., Moen, A., Joosten, H., and Nilsen, N.: The peatland map of Europe, Mires and Peat, 19, pp. 1-17, 2017.

Team, R. C.: A language and environment for statistical computing. Vienna, Austria: R Foundation for Statistical Computing; 2012, URL https//www. R-project. org, 2019.

Tiemeyer, B., Albiac Borraz, E., Augustin, J., Bechtold, M., Beetz, S., Beyer, C., Drösler, M., Ebli, M., Eickenscheidt, T., and Fiedler, S.: High emissions of greenhouse gases from grasslands on peat and other organic soils, Global change
760 biology, 22, 4134-4149, 2016.

Tiemeyer, B., Freibauer, A., Borraz, E. A., Augustin, J., Bechtold, M., Beetz, S., Beyer, C., Ebli, M., Eickenscheidt, T., and Fiedler, S.: A new methodology for organic soils in national greenhouse gas inventories: Data synthesis, derivation and application, Ecological Indicators, 109, 105838, 2020.

Tiggeloven, T., De Moel, H., Winsemius, H. C., Eilander, D., Erkens, G., Gebremedhin, E., Loaiza, A. D., Kuzma, S., Luo,
765 T., and Iceland, C.: Global-scale benefit–cost analysis of coastal flood adaptation to different flood risk drivers using structural measures, Nat. Hazards Earth Syst. Sci, 20, 1025-1044, 2020.

Van Beek, C., Pleijter, M., and Kuikman, P.: Nitrous oxide emissions from fertilized and unfertilized grasslands on peat soil, Nutrient cycling in agroecosystems, 89, 453-461, 2011.

Van den Akker, J., Beuving, J., Hendriks, R., and Wolleswinkel, R.: Maaivelddaling, afbraak en CO2 emissie van Nederlandse
770   veenweidegebieden, Leidraad Bodembescherming, afl, 83, 83, 2007.

Van den Akker, J., Kuikman, P., De Vries, F., Hoving, I., Pleijter, M., Hendriks, R., Wolleswinkel, R., Simões, R., and Kwakernaak, C.: Emission of CO2 from agricultural peat soils in the Netherlands and ways to limit this emission, Proceedings of the 13th International Peat Congress After Wise Use–The Future of Peatlands, Vol. 1 Oral Presentations, Tullamore, Ireland, 8–13 june 2008, 2010, 645-648,

775   Van den Born, G., Kragt, F., Henkens, D., Rijken, B., Van Bemmel, B., Van der Sluis, S., Polman, N., Bos, E. J., Kuhlman, T., and Kwakernaak, C.: Dalende bodems, stijgende kosten: mogelijke maatregelen tegen veenbodemdaling in het landelijk en stedelijk gebied: beleidsstudie, Planbureau voor de Leefomgeving, 2016.

Veenendaal, E., Kolle, O., Leffelaar, P., Schrier-Uijl, A., Van Huissteden, J., Van Walsem, J., Möller, F., and Berendse, F.: CO 2 exchange and carbon balance in two grassland sites on eutrophic drained peat soils, 2007.

780   Ward, S. E., Smart, S. M., Quirk, H., Tallowin, J. R., Mortimer, S. R., Shiel, R. S., Wilby, A., and Bardgett, R. D.: Legacy effects of grassland management on soil carbon to depth, Global change biology, 22, 2929-2938, 2016.

Wilson, D., Blain, D., Couwenberg, J., Evans, C., Murdiyarso, D., Page, S., Renou-Wilson, F., Rieley, J., Sirin, A., and Strack, M.: Greenhouse gas emission factors associated with rewetting of organic soils, Mires and Peat, 17, 2016.